Rochester Institute of Technology
RIT Digital Institutional Repository

Theses

9-2016

A Study on Process, Strength and Microstructure Analysis of Low Temperature SnBi-Containing Solder Pastes Mixed with Lead-free Solder Balls

Sakthi Cibi Kannammal Palaniappan
sk8186@rit.edu

Follow this and additional works at: https://repository.rit.edu/theses

Recommended Citation

Kannammal Palaniappan, Sakthi Cibi, "A Study on Process, Strength and Microstructure Analysis of Low Temperature SnBi-Containing Solder Pastes Mixed with Lead-free Solder Balls" (2016). Thesis. Rochester Institute of Technology. Accessed from

This Thesis is brought to you for free and open access by the RIT Libraries. For more information, please contact repository@rit.edu.

A Study on Process, Strength and Microstructure Analysis of Low Temperature SnBi-Containing Solder Pastes Mixed with Lead-free Solder Balls

by

Sakthi Cibi Kannammal Palaniappan

A Thesis Submitted in Partial Fulfillment of the Requirements for the Degree of
Master of Science in Manufacturing and Mechanical Systems Integration

Supervised by

Dr. Martin K Anselm
Department of Manufacturing and Mechanical Engineering Technology
College of Applied Science and Technology
Rochester Institute of Technology
Rochester, NY
September 2016

Approved by:

____

Dr. Martin K Anselm

Primary Advisor – R.I.T. Dept. of Manufacturing and Mechanical Engineering Technology

____

Dr. James Lee

Secondary Advisor – R.I.T. Dept. of Manufacturing and Mechanical Engineering Technology

____

Dr. Duane Beck

Secondary Advisor – R.I.T. Dept. of Manufacturing and Mechanical Engineering Technology

Dedication

I would like to dedicate this thesis to my parents Mr. S. K. Palaniappan and Mrs. P. Kannammal who have supported me from the beginning of this journey. I would also like to dedicate this to my mentor Dr. Martin K Anselm who has been a great source of motivation and inspiration. Last but not the least, I would dedicate to The God himself who has carried me, guided me and forgiven me numerous times.

Acknowledgements

I take this opportunity to express my profound gratitude and deep regards to my primary advisor Dr. Martin K Anselm for his exemplary guidance, monitoring and constant encouragement throughout this thesis. Dr. Anselm dedicated his valuable time to review my work constantly and provide valuable suggestions that helped in overcoming many obstacles and keeping the work on the right track.

I would like to thank Professor Rich Hailstone for helping me with Scanning Electron Microscope and Professor Surendra Gupta for the help with using optical microscope. I would also like to thank CEMA lab manager Jeffery Lonneville for training me with ball shear test and other equipment in the lab. I would like to thank Universal Instruments Corporation for providing us Cu-OSP test boards and stencil.

Abstract

As the traditional eutectic SnPb solder alloy has been outlawed, the electronic industry has almost completely transitioned to the lead-free solder alloys [1] [2]. The conventional SAC305 solder alloy used in lead-free electronic assembly has a high melting and processing temperature with a typical peak reflow temperature of 245°C which is almost 30°C higher than traditional eutectic SnPb reflow profile. Some of the drawbacks of this high melting and processing temperatures are yield loss due to component warpage which has an impact on solder joint formation like bridging, open defects, head on pillow [3], and other drawbacks which include circuit board degradation, economic and environmental factors [4], and brittle failure defects in the circuit board like pad cratering. To overcome this, a detailed study has been carried out on low temperature lead-free solder paste that utilizes Bi bearing alloys.

Three low temperature lead-free solder pastes, Sn-58Bi, Sn-57Bi-1Ag and Sn-40Bi-Cu-Ni with the melting temperatures of 138°C (which is 45°C below eutectic SnPb and 79°C below SAC) were printed on Cu-OSP finish test boards. These pastes were then assembled with SAC305, Sn99CN and Sn100C solder spheres. The range of Bi concentrations for various mixtures used in this study was calculated to be in the range of 2 to 4 wt%. The mixtures were reflowed under two different low temperatures reflow profiles; (a) a traditional SnPb profile with a peak temperature 217°C and (b) a low temperature SnBi profile with a peak temperature 177°C (recommended by the paste manufacturer). After the assembly process, the mixed solder joints were shear tested to study the failure modes and shear strength at rate of 27.50mils/sec. Cross sectioning was performed to evaluate the possible microstructural changes at room temperature and after aging conditions that may have led to the changes in failure mode observed in shear testing. The isothermal aging condition used in the study is 125°C for 200 hours, which mimics

21 years of field storage at 25°C degrees using Arrhenius extrapolation for Cu_6Sn_5 intermetallic formation. Our study suggests that high temperature reflow profile (217°C peak profile) had better mechanical strength than the low temperature reflow profile (177°C peak profile). A metallurgical explanation for the improvement is presented in this paper. Thus, this paper describes that by generating a robust reflow assembly process for SnBi solder paste, the shear strength can be increased, cost of manufacturing can be reduced and high temperature assembly process (SAC) issues can be minimized which may improve product yield in production.

Table of Contents

Dedication ii

Acknowledgements iii

Abstract iv

List of Figures viii

List of Tables x

1.0 Chapter 1 – Introduction 1

1.1 Why Bismuth based Solder Alloys 4

2.0 Chapter 2 - Experimental Approach 7

2.1 Solder Alloys Used...7

2.2 Board Details.. 7

2.3 Reflow Oven 9

2.4 Thermal Profiling 9

A) High Temperature Reflow Profile 15

B) Low Temperature Reflow Profile.. 16

2.5 BGA on Solder Paste attachment 17

2.6 Sample Solder Mixture Calculation 20

2.7 Shear Test.. 24

2.8 Box Plot Graph.. 26

2.9 Statistical Analysis 27

2.10 Aging Treatment and Micro structural Analysis 30

2.11 Cross Sectioning Analysis 32

2.12 Optical Microscope 32

2.13 Scanning Electron Microscope (SEM) Analysis 34

2.14 IMC Growth Evaluation 37

3.0 Chapter 3 - Results and Discussion 38

A) Sn99CN Process 38

B) Sn100C Process 42

C) SAC Process 46

3.1 Failure Analysis 50

4.0 Chapter 4 - Conclusion 67

References 69

List of Figures

Figure 1 -Cu-OSP test board 8

Figure 2 - Ramp-Soak-Spike Reflow Profile 10

Figure 3 - Ramp-to-Spike Reflow Profile 11

Figure 6 - High Temperature Reflow Profile 15

Figure 7 - Low Temperature Reflow Profile 16

Figure 8 - Solder ball after reflow for shear testing 19

Figure 9 - Shear tool before solder ball 26

Figure 10 - Box Plot Summary 27

Figure 11 - Working Principle of Optical Microscope 34

Figure 12 - Working Principle of Scanning Electron Microscope 37

Figure 13 - IMC Growth Thickness Measurement 38

Figure 14 - Box plot containing shear strength of Sn99CN process in after reflow condition 40

Figure 15 -Box plot containing shear strength of Sn99CN process in aged condition 41

Figure 16 - Box plot containing shear strength of Sn100C process in after reflow condition 44

Figure 17 - Box plot containing shear strength of Sn100C process in aged condition 45

Figure 18 - Box plot containing shear strength of SAC305 process in after reflow 48

Figure 19 - Box plot containing shear strength of SAC305 process in aged condition 49

Figure 21 - Cross section of L20+SAC305 a) Low temperature reflow Profile b) High temperature reflow profile 51

Figure 22 - Cross Polarized Image of L20+SAC305 a) Low temperature reflow Profile b) High temperature reflow profile 52

Figure 23 - Cross section of L23+Sn100C a) Low temperature reflow Profile b) High temperature reflow profile 53

Figure 24 -Cross Polarized Image of L23+Sn100C a) Low temperature reflow Profile b) High temperature reflow profile 53

Figure 25 - Cross section of L27+Sn99CN a) Low temperature reflow Profile b) High temperature reflow profile 54

Figure 26 - Cross Polarized Image of L27+Sn99CN a) Low temperature reflow Profile b) High temperature reflow profile 54

Figure 27 - Low Magnification Image of L27+SAC305/Low Temp Profile/Aged 58

Figure 28 - Sheared Surface of L27+SAC305/Low Temp Profile/Aged 58

Figure 29 - Crack Propagation post Shear Test of L27+SAC305/Low Temp profile/Aged 59

Figure 30 - L20+SAC305/Low Temp profile - Brittle Failure Mode.. 59

Figure 31 - EDS Analysis of L27+SAC305/Low Temp profile/Aged condition 60

Figure 32 - Elemental Mapping of L27+SAC305/Low Temp profile/Aged 61

Figure 33 - a) Low Magnification Image of L27+SAC305/High Temp/Aged b) Sheared Surface of L27+SAC305/High Temp/Aged 62

Figure 34 - Sheared Surface of L27+SAC305/High Temp profile/Aged 62

Figure 35 -Elemental Mapping of L27+SAC305/High Temp profile/Aged 63

Figure 36 - a) L23+Sn99CN/High temperature profile - Dual Failure Mode b) L27+SAC305/High temperature profile - Pad Cratering Failure 64

Figure 37 - Failure modes after reflow 65

List of Tables

Table 1 - List of Solder Alloys used in the study 7

Table 2 - Board Dimensions 8

Table 3 - Zone Temperatures of SnPb Reflow Profile 15

Table 4 - Zone Temperatures of Low Temperature SnBi Paste 16

Table 5 - Recommended Reflow Specifications... 16

Table 6 - The Actual Reflow Specifications 17

Table 7 - Solder sphere size and nominal pad diameter on which solder sphere are placed. 18

Table 8 - Resulting Solder Mixture Composition after reflow 24

Table 9 - Ball Shear Test Parameters.. 25

Table 10 - Sn99Cn Process 39

Table 11 -Mean shear strength of Sn99CN process before and after aging conditions................ 42

Table 12 - Sn100C process 43

Table 13 - Mean shear strength of Sn100C process before and after aging conditions................ 46

Table 14 - SAC305 process 46

Table 15 - Mean shear strength of SAC305 process before and after aging conditions............... 49

Table 16 -Microstructure Evaluation 56

Table 17- IMC growth comparison between as-soldered condition and aged condition 66

1.0 Chapter 1 - Introduction

Solder alloy is the key constituent in the printed circuit board assembly process since it is used to join the electronic components to the board. The solder alloy initially used by the industry was eutectic SnPb alloy (63Sn-37Pb). It is known as eutectic solder because there is no pasty range i.e. the solder alloys melts and solidifies at single temperature (here 183°C) [5] [6]. The solder joint formed should be strong and reliable in terms of electrical connection, mechanical strength and have good thermal properties [7]. Eutectic SnPb was an ideal solder alloy since it performs well in wetting a wide range of PCB surface finishes, has a melting point well above most electronics operational temperatures and exhibits excellent reliability in a variety of stress conditions.

Due to environmental and human health related issue regarding the toxicity of lead, the WEEE (The Waste Electrical and Electronic Equipment Directive) and the RoHS (The Restriction of Hazardous Substances Directive) legislation has banned lead in solder alloys and significant research and development was carried out on lead-free solder alloy alternatives. Considerable research has been conducted on electronics devices processed with lead-free solder alloys and their performance as compared to SnPb in accelerated life testing and processing conditions [8] [9] [10] [11] [12]. Before the introduction of lead-free assembly process the electronic industry has been using the tin-lead solder alloy because of the advantages like low melting temperature, good wettability, solder joint reliability, ease of handling and low cost. After the RoHS legislation, leading researches were carried out and many lead-free solder alloys were suggested as a potential replacement for SnPb solder. The most promising suggestion were solder alloys with tin and copper, tin and silver, and tin, silver and copper(SAC alloy) [13]. As the electronics industry depends on outsourcing to contract manufacturers, a single replacement of SnPb solder alloys is

prioritized in order to have an advantage of standardization. So NEMI and IPC recommended SAC305 alloy [Sn(96.5wt%) Ag(3wt%) Cu(0.5wt%)] as the replacement for SnPb as it was considered to be the next most reliable solder alloy because of its good wetting and mechanical properties [14] [15].

SAC solder alloys have gained acceptance as the most used solder alloys in the electronic industry. There are various compositions of SAC alloys like SAC105[Sn(98.5wt%) Ag(1wt%) Cu(0.5wt%)], SAC305[Sn(96.5wt%) Ag(3wt%) Cu(0.5wt%)], SAC405[Sn(95.5wt%)Ag (4wt%) Cu(0.5wt%)], SACX (low Ag lead-free solder alloy) etc. The addition of silver to the solder alloys has both advantage and disadvantage, which depends on the application and package requirements. Some of the advantage of addition of silver are, it reduces the melting temperature, improves wettability, and results in better thermal fatigue property whereas the disadvantages are poor drop shock performance, higher cost as the percentage of silver in the solder alloy increases and high Cu dissolution rates. [16] [17]

One of the biggest concerns regarding the SAC alloy is the high melting and processing temperatures. Since the SAC alloy has the high temperature assembly process, the intermetallic tends to be thicker as compared to the SnPb process at the solder-substrate interface which can have an effect on the mechanical performance of the solder joint. [18]

The solder material reacts with the substrate material and forms an intermetallic compound layer at the solder substrate interface. The intermetallic growth once formed will continue to grow throughout the life of the solder joint. As the intermetallic layer grows thicker, the solder joint becomes more likely to fail through the intermetallic. This is due to the inherent brittle condition of the crystal like intermetallic as compared to the amorphous solder. Thick intermetallics pose a

reliability risk for the solder joint in case of vibration or any mechanical stress that the substrate is subjected to. The intermetallic layer growth rate is proportional to the temperature and follows the Arrhenius equation; at high temperature the growth rate is faster due to increase in diffusion rates. As the solder melts, the tin will continue to migrate into pad material as long as the temperature is above the melting point. However, the time and temperature should be controlled until the desired wetting is achieved. If the time in which the solder stays liquidus is high, then the dissolution will be high and the intermetallics will continue to grow. One of the studies shows that thickness of intermetallic layer depends on the solder alloy, the surface finish material used and the temperature at which it is maintained [19].

K.Banerji et al. says that high processing temperature creates excessive brittle intermetallic layer which results in weak solder joint formation which is the primary issue in the reliability of BGA packages [20]. One of the study [21] Suh, Daewoong et al. says that the higher yield strength and elastic modulus of SAC alloys results in poor drop shock resistance because it tends to break at the IMC. Another concern about the SAC alloy is the presence of silver in the alloy. Silver being expensive makes it economically less favorable to be used in the consumer electronic products.

An ideal lead-free solder alloy replacement for SnPb solder should meet the following requirements; low melting and processing temperature, good mechanical and thermal properties, good wettability, good thermal properties, non-hazardous, availability of resources and low cost [22] [23].

The electronic industry wants to get rid of lead but at the same time, it does not want high temperature lead-free assembly process. To overcome this, research has been carried out on low temperature lead-free solder alloys. Gallium, Indium, Bismuth, Zinc and Cadmium are just some of the alloying elements which are effective in reducing the melting temperature of solder alloys.

Since cadmium is toxic, it is not considered and Gallium containing alloys are not suitable because they are liquidus at room temperature, too costly and have supply issues. Bismuth and Indium are considered to have similar unique properties, but Indium is much more expensive than any other alloying elements used in solders. Current cost for Indium is approximately $200/kg [24]. Zinc is not considered because of the oxidation issue and brittle nature of the material. Studies show that Sn - Zn based solder alloys have poor wetting properties and they are easily prone to oxidation and corrosion [25] [26] [27] [28]. Therefore, bismuth is a suitable alloying element to reduce the melting temperature. Moreover, the price range of bismuth is similar as tin [24].

A study by J.S Hwang et al. shows that bismuth based alloys has higher yield and tensile strength than SAC alloys. In the Jeong-won Yoon et al. study the eutectic Sn-58Bi solder alloys was shown to have a higher strength and creep resistance than the eutectic Sn-Pb solder alloy [29].

1.1 Why Bismuth based Solder Alloys

SnPb was proven to provide desirable soldering performance and reliability. But, the use of lead in the consumer products has been outlawed by Restriction of Hazardous Substances directive (RoHS) [30]. At present, PCB's that are used in consumer electronic products are assembled with components by reflow soldering with lead-free solder SnAgCu (SAC) which was recommended by NEMI [31] . SAC305 solder alloy has the peak assembly processing temperature range of 240°C to 260°C. Some of the issues with this high temperature SAC solder alloys are:

a) High melting and processing temperatures which necessitated the use of high Tg boards. These high Tg boards are more prone to defects like pad cratering [32].

b) Due to high processing temperature CTE mismatch issue arises which may lead to warpage. This warpage has an impact on solder joint formation like bridging, head on pillow, open defects etc. [33] [34]

c) SAC solder was proved to have fast coarsening of microstructure resulting in degradation of mechanical and thermo-mechanical properties during aging [35]

d) Economic factor is an issue because as the melting point of the solder alloy goes high, the need for high Tg boards and the energy costs in running the reflow oven increases the cost of manufacturing. Environment factors like greenhouse gases emissions are significantly high with the high temperature solder alloy reflow process

To overcome these issues, there has been increasing interest in the research of low temperature lead-free solder alloys. To address this we have carried out a study on low temperature lead-free solder alloys. The base metal for most solders is tin which melts at 235°C. Number of other alloying elements are used to lower the alloys melting temperature. NASA, DOD and other previous researches were carried out with SAC solder containing small amount of Bi was found to reduce the melting temperature to 206°C and improved thermal cycling reliability. This shows that when Bi is added to SAC solder the melting temperature is reduced and the reliability is improved. But these researches were focused mainly on reducing the melting temperature of the solder alloy and they lacked in detailed investigation of mechanical strength, material behavior, failure mechanisms and microstructural analysis. It was also that a risk associated with mixing SnBi paste with SnPb terminated component. It was found that the melting temperature of the resulting could produce a low temperature alloy (96°C melting temperature) which is very low when compared to the operating and processing temperatures of most electronic devices. Finally, one of the studies tells that by adding bismuth, 2 to 4 wt% to tin, tin whisker growth can be reduced to some extent [36].

Currently research is being carried out on low melting point, high concentration bismuth in tin-based solder alloys like Sn-58wt%Bi, Sn-57wt%Bi-1wt%Ag and Sn-40wt%Bi-Cu-Ni. SnBi solder paste is in the market already but one drawback of not using in consumer products has been its brittleness under mechanical shock conditions [37]. A few studies proved that by adding 0.25wt% to 1.0wt% of silver to SnBi binary alloy, can improve the ductility and reduce the brittle deformation behavior of SnBi alloys [38] [39]. Moreover, recent research has revealed that by mixing BGA solder balls with Bi-Sn-Ag solder paste has shown significant reduction in mechanical drop reliability when compared with solder joints formed with SAC solder paste plus SAC ball [40] [41]. However, no paper has discussed the mechanical behavior, or the microstructure of the solder joint and its effect on failure mechanism in mixing SnBi solder paste with the lead-free solder balls.

The objective of this research is to provide the industry with processing recommendation for products that are assembled using high temperature SAC solder balls with low temperature SnBi solder paste.

In this study we have focused on the analysis of mixing lead-free solder spheres like SAC305(Sn-3.0wt%Ag-0.5wt%Cu), Sn100C(Sn-0.7wt%Cu-0.05wt%Ni+Ge) and Sn99CN(Sn-1.1wt%Ag-0.7wt%Cu-0.05wt%Ni+α) with low temperature SnBi solder pastes like L20(Sn-58wt%Bi), L23(Sn-57wt%Bi-1wt%Ag) and L27(Sn-40wt%Bi-Cu-Ni (the wt% of Cu-Ni is less than 1% cumulatively)) manufactured by Senju Metal Industry Co Limited. We have also studied the shear strength and microstructure analysis after cross sectioning to give a better understanding of mixing these lead-free solder balls with low temperature SnBi solder paste in terms of convection reflow process, failure mode, mechanical reliability, IMC growth, and the size and distribution of various precipitates in solder joint formation.

2.0 Chapter 2 - Experimental Approach

2.1 Solder Alloys Used

The list of lead-free solder spheres and the Bi bearing solder pastes used in this study are described in Table 1

Solder Alloy	Composition in Wt%	Melting Point (°C)	Sphere Diameter
SAC 305	Sn/3.0Ag/0.5Cu	215°C	30mils
Sn100C	Sn/0.7Cu/0.05Ni+Ge	227°C	20mils
Sn99CN	Sn/1.1Ag/0.7Cu/0.05Ni+α	227°C	18mils
L20	Sn/58Bi	139°C ~ 141°C	Type 4 -Solder Paste
L23	Sn-57Bi-1Ag	138°C ~ 204°C	Type 4 -Solder Paste
L27	Sn/40Bi-Cu-Ni	138°C ~ 174°C	Type 4 -Solder Paste

Table 1 - List of Solder Alloys used in the study

2.2 Board Details

Universal Instruments Corporation, a global leader in the design and manufacture of advanced automation and assembly equipment for the electronics manufacturing industry, provided one of their soldering test boards. These boards were plated in Cu-OSP surface finish. The board dimensions and thickness are 66 x 66 mm and 2 mm respectively. The board has 7 different pad dimensions with 75 pads for each dimension which are all solder mask defined. The picture of the board is in Figure 1. The nominal and measured pad dimensions are in table 2.

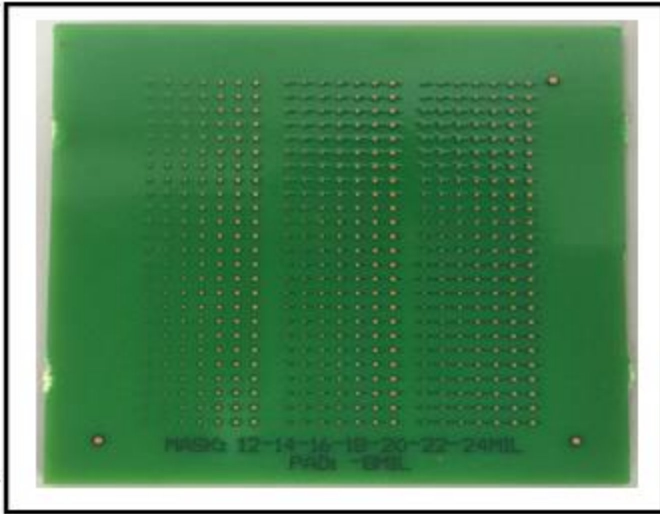

Figure 1 -Cu-OSP test board

Nominal Pad Diameter (mils)	**Measured Pad Diameter (mils)**
12	10.8
14	12.8
16	14.7
18	16.8
20	18.9
22	21.0
24	23.0

Table 2 - Board Dimensions

2.3 Reflow Oven

A reflow profile is the time-temperature relationship of the printed circuit board assembly as it runs through the oven. It is a result of the oven recipe developed for the heating and cooling zones of convection reflow oven. A Heller 1808 MK III convection oven was used for our experimentation. It is a forced convection reflow oven with eight heat zones and two cooling zones. It has a single-rail edge hold conveyor belt that is adjustable to accommodate different board size (max 20 inches wide) and the maximum conveyor speed is 80 centimeters per minute. It is an ISO 9001 CMS certified and lead-free approved machine.

2.4 Thermal Profiling

SlimKIC 2000 is the name of the thermal profiler used to create thermal reflow profile for the test sample used in this experiment. It has 9 thermocouple (TC) channels/inputs which includes a TC for reading air temperature. The KIC profilers have a configuration that can transmit real-time data as it moves in the oven and it can simultaneously record the data internally. When the KIC profiler comes out of the oven, the internally recorded profile data is wirelessly downloaded into the screen as real-time profile. SlimKIC software has the powerful feature called PWI (Process Window Index). This tool ranks the generated thermal profile and tells how it fits the standard profile given by solder manufacturer. The center of the process window is set to be zero and the extreme edges are +/- 99%. When this exceeds greater than +/-100% it tells that the profile is out of process specifications. The calculation for PWI is explained in detail in the next section in Figure 5.

There are two types of reflow profile a) Ramp-Soak-Spike and b) Ramp-to-Spike.

The Ramp-Soak-Spike profile has four zones: Ramp up, Soak, Spike and Ramp down. Ramp is defined as the rate of change in temperature (°C) over time (seconds). The soak zone is to bring the

component and PCB to equilibrium stage in terms of heat energy so that thermal shock can be prevented. The spike zone is where the time above liquidus is calculated for a given temperate range i.e. the time exceeding the melting point of the alloy. The figure of ramp-soak-spike profile is shown in Figure 2 below.

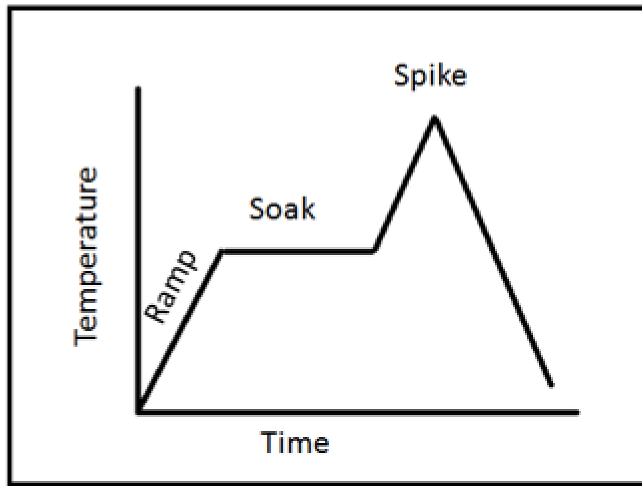

Figure 2 - Ramp-Soak-Spike Reflow Profile

The ramp down zone is the cooling section. The Ramp-to-Spike profile has 3 zones. The profile looks like a linear graph with a ramp up zone to spike and then ramp down. There is no soak zone and the soak here is controlled by the conveyor speed. The reflow profile used in our study is the ramp-to-spike profile. The figure of ramp-to-spike profile is shown in Figure 3 below.

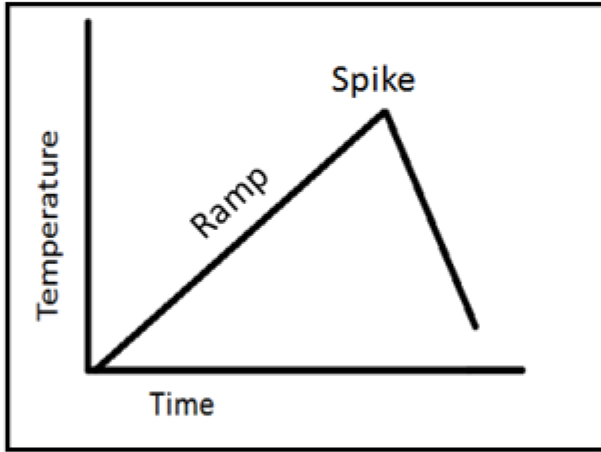

Figure 3 - Ramp-to-Spike Reflow Profile

The profile in figure 4 below shows the comparison of lead-free solder and SnPb solder alloys. It can be seen from the profile that lead-free profile as higher temperature than the SnPb profile profile. The melting point of SnPb is 183°C and for the lead-free solder alloy (here SAC305) is 215°C. The differences in the melting point between these two profiles are 34°C. The peak temperature for the SnPb profile is 220°C and the peak temperature for the lead-free solder alloys is 260°C. The differences in the peak temperature between these two profiles are 40°C. This clearly shows that the SAC305 alloy has higher processing temperature than SnPb profile. To reduce this higher processing temperature, low melting SnBi solder alloys are used.

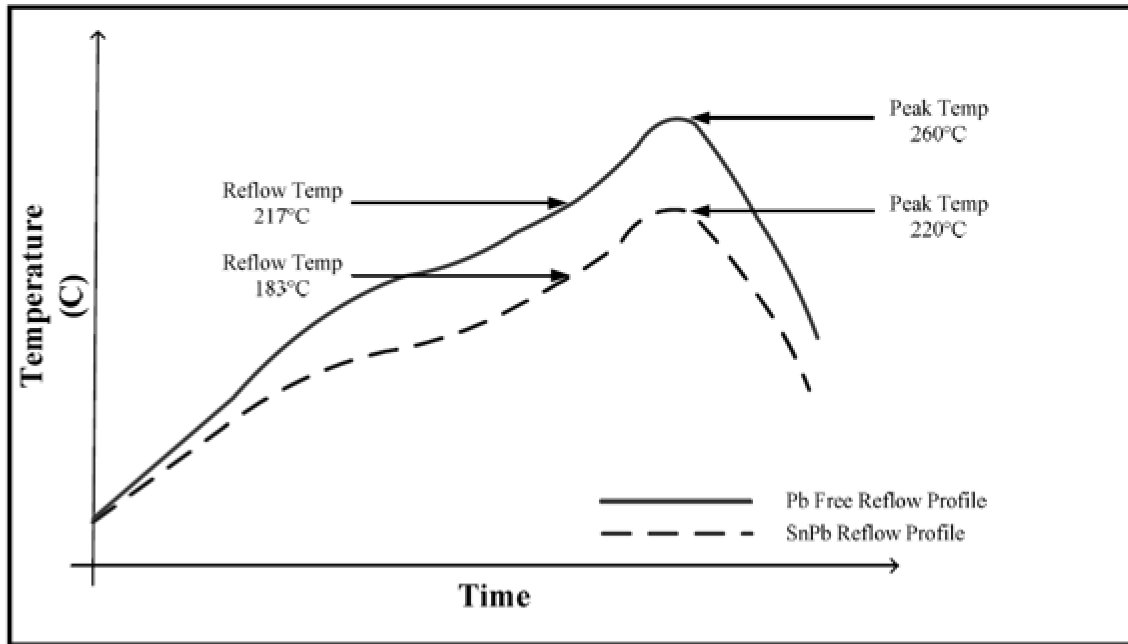

Figure 4 - Comparison of Lead-free and High temperature profile

To start the reflow profiling, thermocouple is attached on the pad. The Heller oven is allowed to heat until all zones reaches its set temperatures. Then the test boards with the thermocouples attached in it are sent to the reflow machine and desired profile was generated. The generated profile was analyzed and necessary changes were made on the zone temperatures until we get the optimum profile that relates to the solder alloy used.

The following are the parameter that needs to be considered for the reflow profiling: maximum rising slope, maximum falling slope, reflow time (time above liquidus), peak temperature, conveyor speed and process window index.

1) Maximum Rising Slope - It is the rate of change in rising temperature to time which is expressed in degrees per second.

2) Maximum Falling Slope - It is the rate of change in falling temperature to time which is expressed in degrees per second.

3) Time Above Liquidus (TAL) - It is the time exceeding the melting point of the alloy over certain temperature range. It is expressed in seconds.

4) Peak Temperature - It is the maximum temperature the board undergoes during the reflow profile. It is expressed in degree centigrade.

5) Conveyor Speed - It is the speed at which the conveyor rail runs inside the reflow oven. It is expressed in centimeters per minute.

6) Process Window Index (PWI) - PWI is a statistical tool that comes with SlimKIC software. PWI is a measure that tells how well a profile fits the user defined process limits. It compares the generated reflow profile with the standard reflow profile given by solder manufacturer and shows how good the generated profile is in terms of standard specification. It is expressed in percentage. The profile is considered good if the PWI is between +/- 99%. If PWI exceeds more than this then the process is not acceptable. For example, if four thermocouple are used for running a profile and four profile statistic are logged for each thermocouple then there would be 16 statistic for that profile and the PWI will be the worst case i.e. the highest number expressed as percentage in that set of profile statistics. The Figure 5 below shows four statistics like slope, soak time, peak temperature and time above liquidus. The PWI is calculated for individual statistic using the formula below and it is found to be 0%, 20%, 60% and 40% respectively and the overall PWI for the profile is 60% (highest number expressed as percentage).

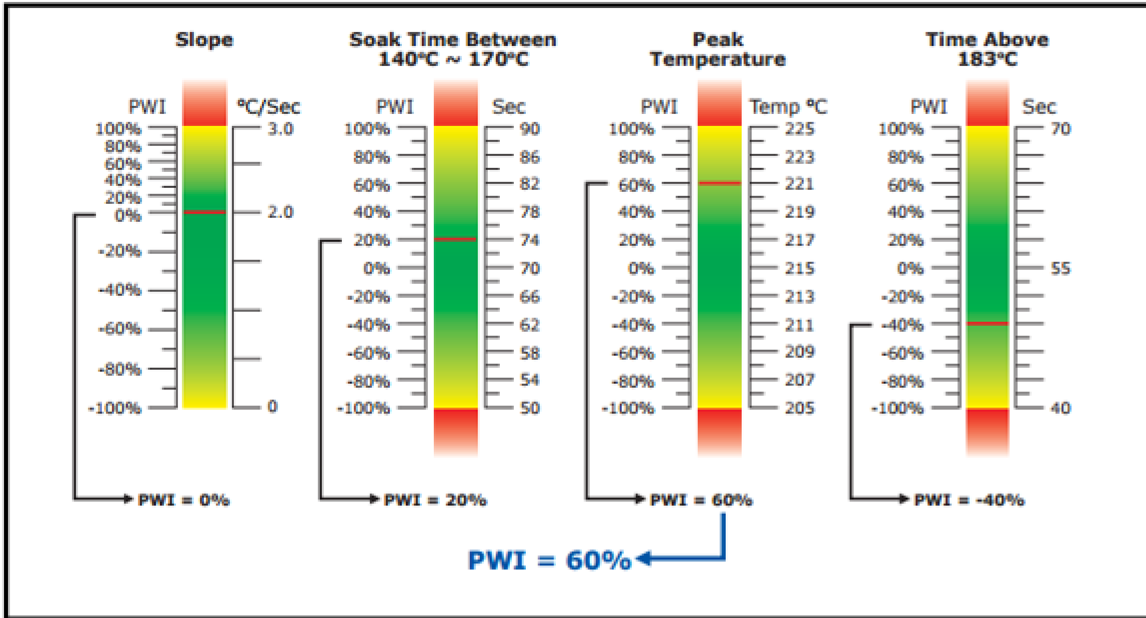

Figure 5 -PWI Calculation

The formula for Process Window Index calculation (PWI) [42] is as follows,

$$\mathbf{PWI} = 100 \times \underset{N,M}{\overset{i,j=1}{\mathrm{MAX}}} \left\{ \left| \frac{(\text{measured value}_{[i,j]} - \text{average limits}_{[i,j]})}{(\text{range}_{[i,j]} / 2)} \right| \right\}$$

i =1 to N (number of thermocouples)

j = 1 to M (number of statistic per thermocouple)

Measured $\text{value}_{[i,j]}$ =$[i,j]^{th}$ statistic's value

Average $\text{limits}_{[i,j]}$ = average of the $[i,j]^{th}$ statistic's high and low limits

$\text{Range}_{[i,j]}$ = $[i,j]^{th}$ statistic's high limit minus the low limit

Now, let us see the generated reflow profile of low temperature and high temperature (SnPb) reflow profile process. The zone temperatures of the profile and its parameters are in Table 3 and

Table 4. The reflow profile of low temperature and high temperature reflow profile are shown in Figure 4 and Figure 5.

A) High Temperature Reflow Profile

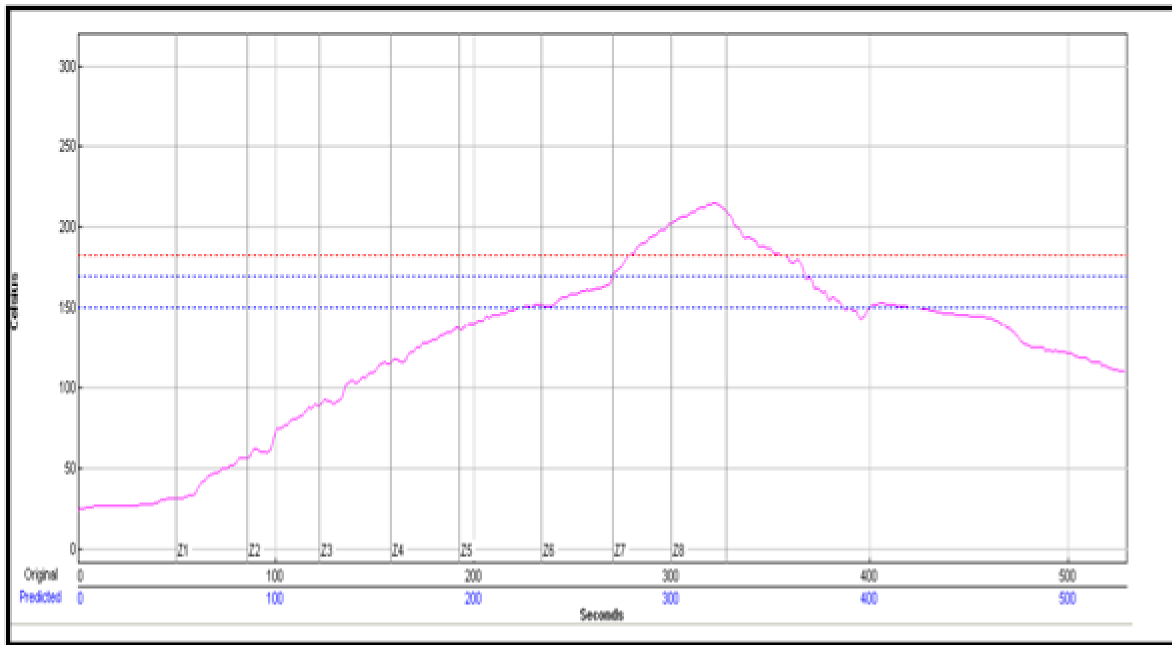

Figure 4 - High Temperature Reflow Profile

Zone	Z1	Z2	Z3	Z4	Z5	Z6	Z7	Z8	Conveyor Speed - 54.0cm/min	PWI - 60%
Temp(°C)	90	95	100	135	138	138	195	200		

Table 3 - Zone Temperatures of High Temperature Reflow Profile

B) Low Temperature Reflow Profile

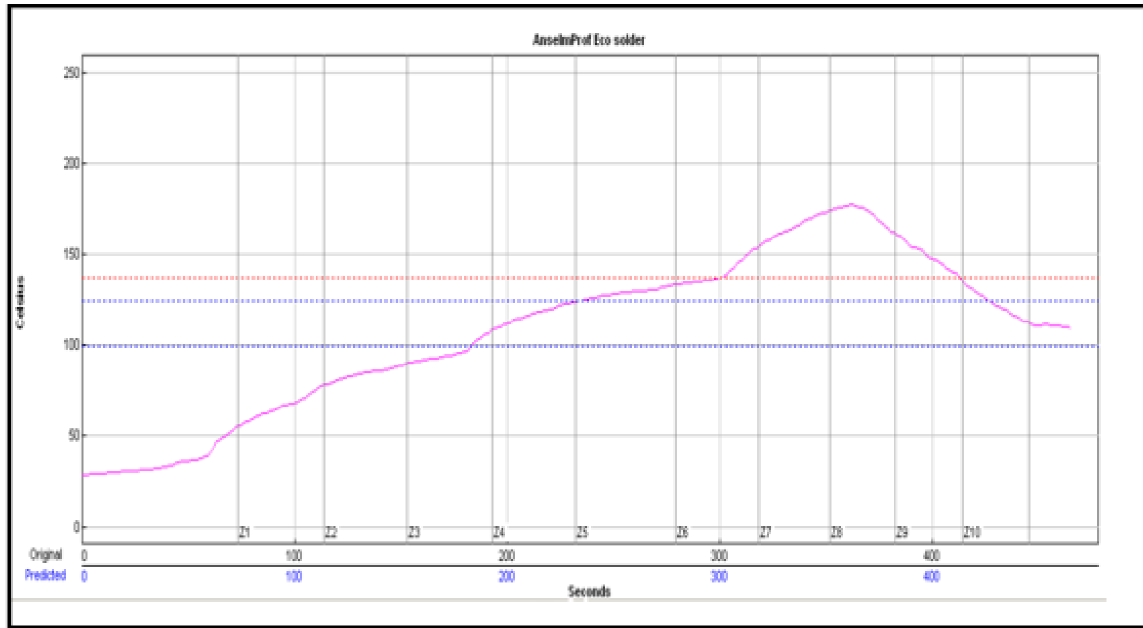

Figure 5 - Low Temperature Reflow Profile

Zone	Z1	Z2	Z3	Z4	Z5	Z6	Z7	Z8	Conveyor Speed-	PWI - 73%
Temp(°C)	90	120	150	165	175	175	255	260	47.0 cm/min	

Table 4 - Zone Temperatures of Low Temperature Paste

The solder manufacturers recommended reflow specification for high temperature and low temperature reflow profile is as follows in Table 5

Reflow Profile	**Max Rising Slope (°C/seconds)**	**Soak Time (seconds)**	**Peak Temp (°C)**	**Time Above Liquidus (seconds)**
High Temp	0 - 1.5	0 - 60	205 - 225	30 - 90
Low Temp	0 - 2	0 - 60	165 - 200	60 - 120

Table 5 - Recommended Reflow Specifications

The actual generated reflow profile specification for high temperature and low temperature process is shown in Table 6 below. All the reflow parameters are within the specification given by the solder manufacturers and the process window index of both the profiles are with the acceptable range.

Reflow Profile	Max Rising Slope (°C/seconds)	Soak Time (seconds)	Peak Temp (°C)	Time Above Liquidus (seconds)
High Temp	1.45	48	217	76
Low Temp	0.98	50	177	101

Table 6 - The Actual Reflow Specifications

2.5 BGA on Solder Paste attachment

Once the desired profile were generated, the SnBi solder paste are printed using a stencil and lead-free solder spheres are populated on the paste deposited. Three low-temperature solder pastes Bi-42Sn, Sn-57Bi-1Ag and Sn-40Bi-Cu-Ni with the melting point of 138°C are deposited using stencil and squeegee on the Cu-OSP finish test boards. A stencil is used in order to get uniform solder paste deposition in the entire pad. Thickness of the stencil used is 4.33 mils. Then, SAC 305, Sn100C and Sn99CN solder spheres are placed on the solder paste deposited manually using tweezers and the microscope. The solder spheres are placed on considerably smaller pads so that it will provide an ideal shape to the soldered sphere for shear testing. The Table 7 below shows the size of the solder sphere and the nominal pad diameter on which it is placed.

Solder Sphere	**Solder Sphere Size (mils)**	**Nominal pad diameter on which solder sphere are placed (mils)**
SAC305	30	24
Sn100C	20	14
Sn99CN	18	12

Table 7 - Solder sphere size and nominal pad diameter on which solder sphere are placed

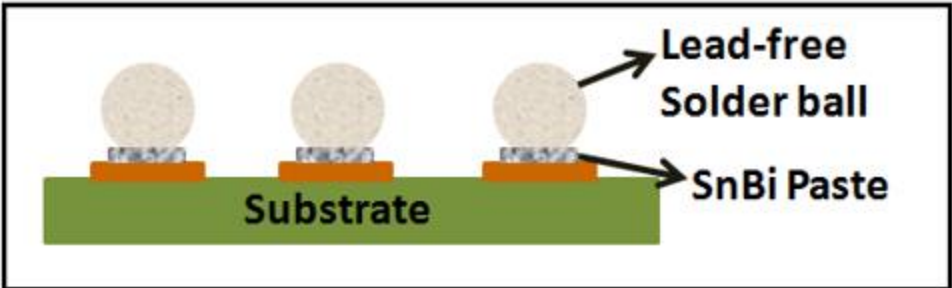

Figure 6 - Mixed Solder Alloy – SnBi paste + Lead-free balls

After populating the boards with solder spheres, it is then sent into the reflow oven. Two different reflow profiles were used, a) High temperature profile (Eutectic Tin-Lead profile with the melting temperature of 183°C, peak temperature of 217°C and time above liquidus (TAL) of 73 seconds) and b) Low temperature profile (SnBi reflow profile with the melting temperature of 138°C, peak temperature of 176°C and TAL of 111.6 seconds). Comparison is done with the traditional SnPb (Here high temperature profile), because it is considered as the standard profile earlier. Shear testing was done to study the mechanical strength of the mixed solder alloy. The Figure 7 below shows the solder ball after reflow for shear testing.

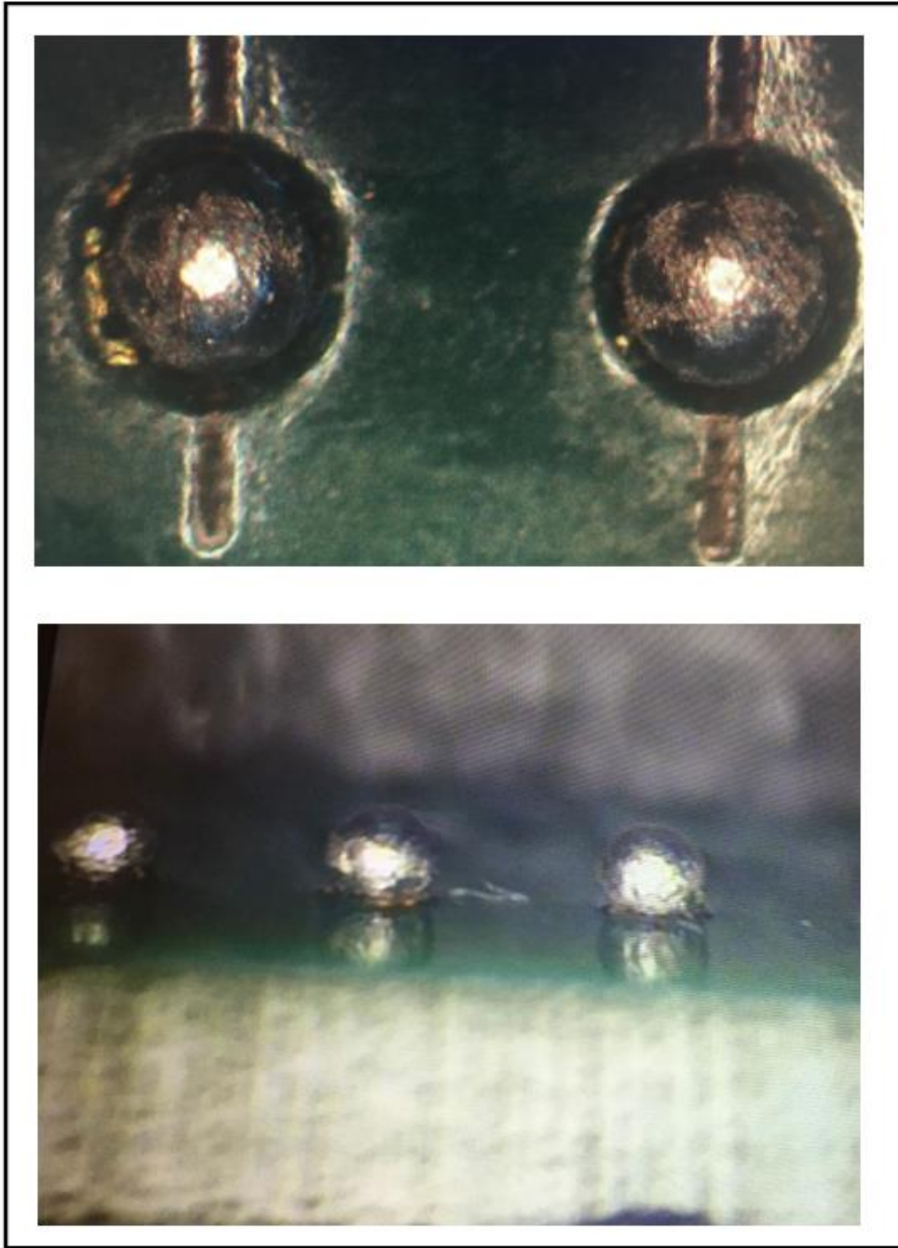

Figure 7 - Solder ball after reflow for shear testing

2.6 Sample Solder Mixture Calculation

Volume of L20 paste - $\pi r^2 h$

r – Radius of the stencil (10.8 mils)

h – Thickness of the stencil (4.33 mils)

Volume of L20 paste = $\pi \times (0.0108)^2 \times 0.00433$ (1 mil = 0.001inch)

$= 1.59 \times 10^{-6}$ inch^3

$= 2.6 \times 10^{-5}$ cm^3 (1 inch^3 = 16.387 cm^3)

Volume of SAC305 ball = $\frac{4}{3} \pi r^3$

r – Radius of the SAC305 sphere (30 mils)

$= \frac{4}{3} \times \pi \times (0.015)^3$

$= 1.4 \times 10^{-5}$ inch^3 (1 mil = 0.001inch)

$= 2.3 \times 10^{-4}$ cm^3 (1 inch^3 = 16.387 cm^3)

Density X Volume = Mass

For L20 - 8.62 g/cm^3 x (2.6x10^{-5}cm^3 x 50%) = 0.000112g (Type 4 Solder Paste = 50% Solder Wgt, 50% flux wgt)

Mass, m1= 0.112mg ----- (1)

For SAC305 – 7.39 g/cm^3 x 2.3x10^{-4}cm^3 =0.00171g

Mass, m2 = 1.71mg ----- (2)

Total Mass = m1+m2 = 1.822mg ----- (3)

Composition L20 Paste - Sn - 42 wt%

Bi - 58 wt% ----- (4)

Composition of SAC305 ball - Sn - 96.5 wt%

Ag - 3.0 wt%

Cu - 0.5 wt% ----- (5)

By multiplying individual composition of L20 paste (equation 4) to the mass of L20 paste (equation 1), we get weight in mg of L20Paste.

Bi - 0.065 mg

Sn - 0.047 mg ----- (6)

Similarly, by multiplying individual composition of SAC305 ball (equation 5) to the mass of SAC305 ball (equation 2) we get weight in mg of SAC305 ball.

Sn - 1.650 mg

Ag - 0.0513 mg

Cu - 0.00855 mg ----- (7)

Adding equation (6) and equation (7) we get the weight in mg of the resulting mixture,

Sn -1.697 mg

Bi - 0.065 mg

Ag - 0.0513 mg

Cu - 0.00855 mg ----- (8)

To get the resulting mixture in wgt %, the individual composition of mixture in equation (8) is divided by total mass in equation (3),

L20 + SAC305 = Sn – 93.14 wt%

Bi – 3.56 wt%

Ag – 2.81 wt%

Cu - 0.47 wt%

Similar calculation is done for other solder paste and solder ball combination and the resulting mixture in weight percentage is calculated which shown in Table 8

Mixed Solder Alloy	**Composition in Wt % of Solder Mixture After Reflow**
L20 + SAC305	Sn - 93.14% Bi - 3.56% Ag - 2.81% Cu - 0.47%
L23 + SAC305	Sn - 93.15% Bi - 3.50% Ag - 2.87% Cu - 0.47%
L27 + SAC305	Sn - 94.31% Bi - 2.33% Ag - 2.82% Cu - 0.5% Ni - 0.029%
L20 + Sn100C	Sn - 95.21%

	Bi - 4% Cu - 0.651% Ni - 0.023% Ge - 0.023%
L23 + Sn100C	Sn - 95.14% Bi - 4% Ag -0.07% Cu - 0.65% Ni - 0.023% Ge - 0.023%
L27 + Sn100C	Sn - 96.55% Bi - 3% Cu - 0.687% Ni - 0.057% Ge - 0.023%
L20 + Sn99CN	Sn - 94.47% Bi - 4% Ag - 1.02% Cu - 0.65% Ni+α – 0.047%
L23 + Sn99CN	Sn - 94.51% Bi - 3.71% Ag - 1.08%

	Cu - 0.65% Ni+α - 0.046%
L27 + Sn99CN	Sn - 95.71% Bi - 2% Ag - 1.03% Cu - 0.68% Ni+α - 0.078%

Table 8 - Resulting Solder Mixture Composition after reflow

2.7 Shear Test

The strength of solder ball joints can be characterized by mechanical ball shear tests. Ball shear testing is a destructive testing method that is used to study the solder joint strength by applying load. As the load propagates through the solder joint plastic deformation occurs and the failure modes are analyzed from the fractured surface [43] [44] [45].

The Nordson Dage 4000 series is a multipurpose bond tester that is used in this study for shear testing. This equipment is capable of performing various pull and shear application like wire bond pull test, ball shear test, die shear test. We have performed solder ball shear test using the bond tester. The reflowed solder balls were sheared individually using the tool and shear force is measured (in grams) throughout the test. The Figure 8 below represents the image of shear tool sitting before solder ball. Fifteen solder balls were sheared for each solder mixture and the readings were noted. Low speed shear test are not used because they are not suitable for evaluation of joint strength under drop loading. 100 kg load cartridge was used with test speed of 27.50 mils/sec and the height of the tool from the PCB is 1 mil. The solder ball shear testing is done in accordance with the JEDEC JESD22-B117 standard. The position of shear tool during shear test is very important

for accurate and repeatable results. The shear height accuracies for this equipment is +/- 0.25 microns. The system accuracy is up to +/- 0.1% of the selected load range. The more precise alignment of the shear tool to the ball is achieved using joystick control. The shear force in grams is converted to Newton's, which is then normalized to MPa. The parameters used for shear testing are as follows in Table 9.

Parameters	**Description**
Load Cartridge	100kg
Range	0 to 5 kg (+/- 1.25)
Test Speed	27.54 mils/sec
Test Load	2000g
Land Speed	19.67 mils/sec
Shear Height	1.5 mil

Table 9 - Ball Shear Test Parameters

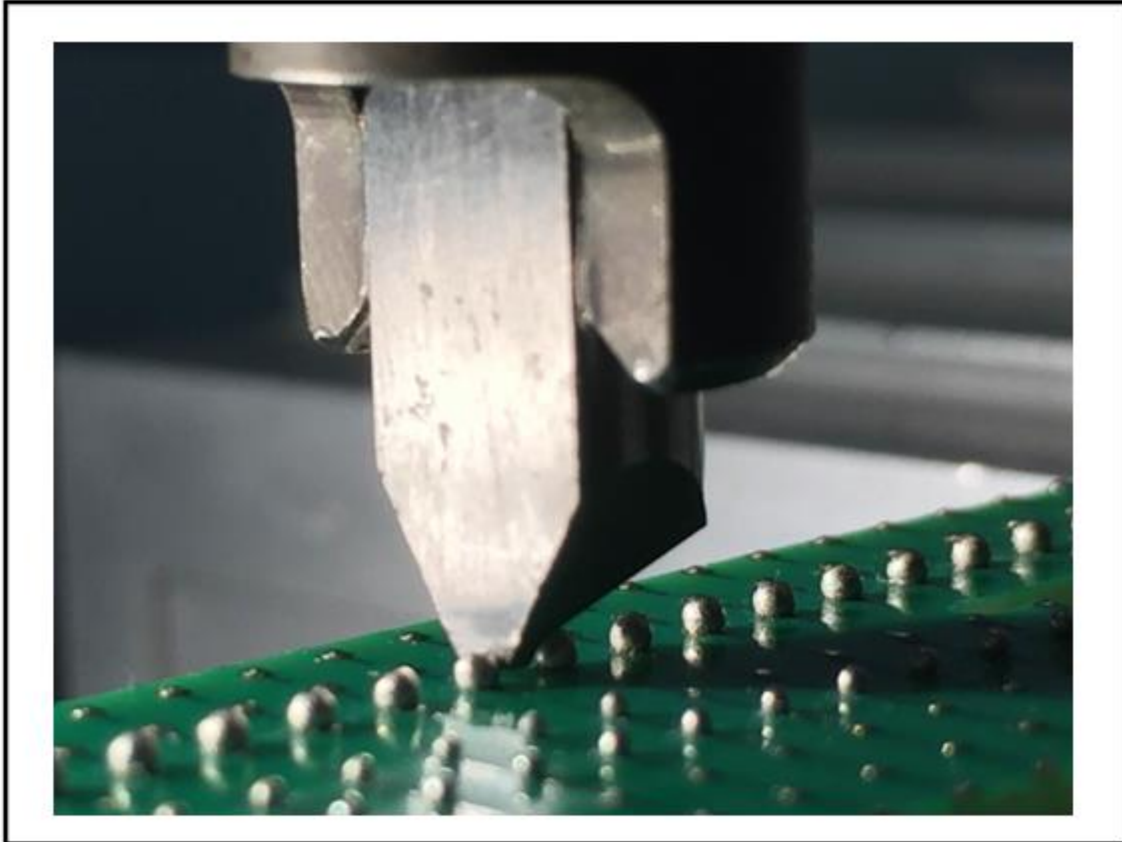

Figure 8 - Shear tool before solder ball

After shear testing, the sheared pad surfaces were analyzed using the microscope to find the type of failure mode that has occurred. There are three kinds of failure modes: Solder failure, dual failure and IMC failure. When the fractured pad surface has 0 to 30% IMC then it is called as solder failure. When it is 30 to 70% IMC, then it is called as dual failure and when it is 70 to 100% IMC then it is called as IMC failure mode.

2.8 Box Plot Graph

A box plot is a summary of distribution of a sample which shows the shape, variability and central tendency (mean, median, mode). It helps in comparing and understanding of various distributions. Box plot graph in this study is generated using the Minitab software for the various

shear forces and the trend in the shear forces are analyzed for two different reflow profiles with different solder mixtures. The box plot graph gives details about the mean, median, variability and the standard deviation of the sample-sheared forces. A sample box plot graph is shown in Figure 9 [46]. The middle line in the box plot is the median, which is where 50% of the value lies. The line below that is lower quartile and it is where 25% of the value lies. The line above the median is the upper quartile and it is where 75% of the value lies. The line above upper quartile is the upper extreme and the line below the lower quartile is the lower extreme. The single point sitting outside the plot represents the outlier.

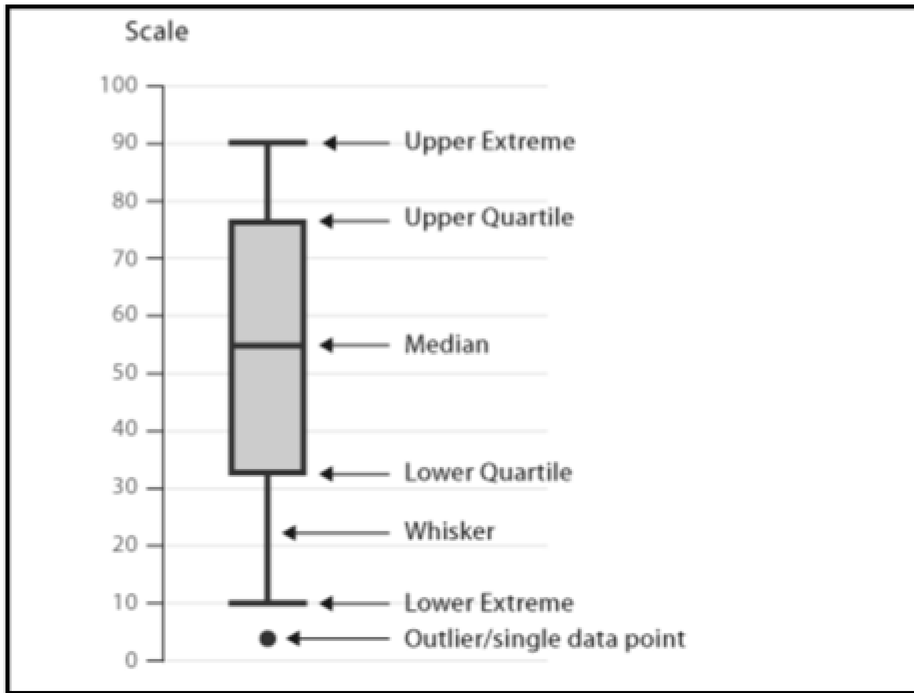

Figure 9 - Box Plot Summary

2.9 Statistical Analysis

2 sample t-test and paired t test statistical analysis were carried out to support the shear strength analysis. Both the t-tests are carried out using the Minitab 16 statistical software.

2 sample t-test

2 sample t-test is carried out to calculate the difference between the population means and to determine if the means of the two independent population are equal. It is type of hypothesis test where the null hypothesis is, the means of the two samples are equal and the alternate hypothesis is, they are not equal. The result of the 2 sample hypothesis test includes the confidence limits for the mean and the P-value. Confidence limits for the mean are interval estimate for the true mean value. A confidence interval generates lower and upper limit for the mean and it tells how much uncertainty is there in our estimate true mean. The tighter the interval, the precise is our estimate. Confidence intervals are shown in terms of confidence level. In our study we have used a confidence level of 95% which means we are confident that 95% of the time, the intervals will contain the true mean. P-value is used to check the hypothesis. Generally, 5% is considered as the alpha risk, which means that there are 5% chances for the mean to be out of the interval. If the P-value is greater than 0.05 then we fail to reject the null hypothesis and if the P-value is less than 0.05 then we reject the null hypothesis. In our study a 2 sample t-test is carried out to check whether the shear strength of paste-ball combinations in two reflow profiles (high temperature and low temperature) are having the same mean. An example of 2 sample t-test result is shown below,

```
Two-sample T for L23+SAC305/Low Temp/30mils(N/mm2)vs L23+SAC305/High
Temp/30mils(N/mm2)

                                 N   Mean  StDev  SE Mean
L23+SAC305/Low Temp /30mils     15  46.65   3.31     0.85
L23+SAC305/High Temp/30mils     15  86.10   5.68      1.5


Difference = μ (L23+SAC305/Bi-Eco/30mils(N/mm2)) - μ (L23+SAC305/SnPb/30mils(N/mm2))
Estimate for difference:  -39.44
95% CI for difference:  (-42.97, -35.92)
T-Test of difference = 0 (vs ≠): T-Value = -23.23  P-Value = 0.000
```

In our test, the null hypothesis is the mean shear strength of two reflow profiles are equal ($\mu_{LowTemp}$ - $\mu_{HighTemp}$=0) and the alternate hypothesis is, the mean shear strength of the two reflow profiles are different ($\mu_{LowTemp}$ - $\mu_{HighTemp} \neq 0$). Where $\mu_{lowTemp}$ is the mean shear strength of paste-ball combinations using low temperature reflow profile and $\mu_{HighTemp}$ is the mean shear strength of paste-ball combinations using high temperature reflow profile.

From the result, we can see that the P-value is less than 0.05, so we reject the null hypothesis which means that there is a significant difference between the two reflow profiles. It can also be said from the confidence interval because the value zero ($\mu_{LowTemp}$ - $\mu_{HighTemp}$ =0) does not lie between the estimated confidence interval (-42.97,-35.92) so we reject the null hypothesis which means that there is a significant difference between the two reflow profiles.

Paired t-test

A paired t-test is carried out to check if the mean of the differences between two paired samples differs from zero. A paired t-test is mostly used for analyzing before-after studies. In our study, we have carried out the paired t-test to determine if there any change in the mean shear strength before and after the aging condition. A paired t-test calculates the difference between before and after aging condition's mean shear strength, determines the difference in the mean, and tells if it is significant. It is also a type of hypothesis testing, where the null hypothesis is the population mean of the difference are equal and the alternate hypothesis is the population mean of the difference is not equal. An example of paired t-test result is shown below,

```
Paired T for Before aging L23+Sn100C/High Temp/20mils(N/mm2) - After aging
L23+Sn100C/High Temp/20mils(N/mm2)

                                N   Mean  StDev  SE Mean
L23+Sn100C/High Temp/20mils    15  83.07   4.97     1.28
AL23+Sn100C/High Temp/20mils   15  85.20  13.57     3.50
Difference                     15  -2.12  16.81     4.34


95% CI for mean difference: (-11.43, 7.18)
T-Test of mean difference = 0 (vs ≠ 0): T-Value = -0.49  P-Value = 0.632
```

In our test, the null hypothesis is the population mean of difference before and after aging are equal ($\mu_{Before\ aging} - \mu_{After\ aging}=0$) and the alternate hypothesis is, the population mean of difference before and after aging are not equal ($\mu_{Before\ aging} - \mu_{After\ aging} \neq 0$). Where $\mu_{Before\ aging}$ is the mean shear strength of paste-ball combinations before aging (here high temperature reflow profile) and $\mu_{After\ aging}$ is the mean shear strength of paste-ball combinations after aging (here high temp reflow profile).

From the result, we can see that the P-value is greater than 0.05, so we fail to reject the null hypothesis which means that the population mean of difference before and after aging are equal. It can also be said from the confidence interval because the value zero ($\mu_{Before\ aging} - \mu_{After\ aging} = 0$) lies between the estimated confidence interval (-11.43, 7.18) so we fail to reject the null hypothesis as the population mean difference before and after aging are not different.

2.10 Aging Treatment and Micro structural Analysis

The solder joints are cross-sectioned for examination immediately after reflow and then after aging process to study and compare the evolution of microstructure over the period of time. Isothermal aging is done to study the consequence and effect of constant prolonged elevated temperature on solder alloys and to study the effect of intermetallics on solder joint reliability. The Arrhenius Equation is used to correlate time in the field at normal use temperature to a Constant Temperature Accelerated Life Test. The Acceleration Factor (AF) calculation is as follows, [47]

$AF = e^{[(-Ea/K)(1/T1-1/T2)}$

T_1 = Field Temperature (K)

T_2 = Test Temperature (K)

$E_a = 0.7eV$

$K = 8.62x10^{-5}$ eV/K (Boltzman constant)

$$\frac{Ea}{K} = 8120.64$$

$$\frac{1}{T1} = \frac{1}{298}$$

$$\frac{1}{T2} = \frac{1}{398}$$

$$\frac{1}{T1} - \frac{1}{T2} = 8.431x10^{-4}$$

$$AF = e^{(8120.64)(8.431x10\text{^}-4)}$$

AF =934.49

Testing at 1000 hours at 125°C is therefore equivalent to 934,490 hours or 106.67 years of life at the normal operating temperature at 25°C. Aging the board for 200 hours (8.33 days) is equivalent to 21.2 years. To mimic end of life conditions, isothermal aging of our sample solder joints were aged at 125°C for 200 hours.

2.11 Cross Sectional Analysis

Cross sectional analysis was done to evaluate the following: Dissolution of SnBi paste on lead-free solder balls, grain boundary orientation using cross polarized images, intermetallic growth in the as-soldered and isothermal aged conditions, change of failure mode in shear testing in the as-soldered and isothermal aging condition, and the size and distribution of various precipitates in the solder joint formation using Scanning Electron Microscope (SEM). The samples were molded in an epoxy resin for cross sectioning. Grinding and polishing were done using diamond based suspension particles (up to 1 micro meter particle size).

Struers Tegraforce 5 was the equipment used for cross sectioning samples. The Tegraforce 5 is fully automatic and it is capable of holding up to 6 specimens. The samples to be cross-sectioned are molded in an epoxy resin, and were ground and polished using diamond based suspension particles. Grinding removes particles on the sample, by which it levels and cleans the sample surface. Silicon carbide grit paper number 500 and 1000 were used for grinding. Polishing removes the micro particles and the marks formed during the grinding process. 15, 9, 3, 1 micrometer particles were used to prepare the samples for optical microscopy.

2.12 Optical Microscope

The optical microscope used in this experiment is Olympus bx60m which is a compound microscope with two or more lenses. The eyepiece lens is 10X and the objective lenses are 5X, 10X, 20X, 50X, 100X. This microscope is capable of capturing bright field, dark field and cross-polarized images. In this study, we have used bright field images for dissolution analysis and cross-polarized images for grain morphology analysis. The optical microscope is a type of microscope which utilizes the light and some of the lenses to magnify images of the samples. The Figure 10 below illustrates the working principal of an optical microscope [48]. The main components of the

optical microscope are ocular lens, objective lens, specimen stage and the light source. The ocular lens is in the eyepiece and the objective lenses are in the revolving nosepiece which is near the specimen sample. The specimen stage is where the specimen sample is held and the light source is below the specimen stage. This microscope gets the light from the light source and sends it through the objective lens which magnifies the samples and sends it to the eyepiece. This eyepiece which has the ocular lens of 10X magnification further magnifies the sample and gives the virtual image to the eyes. To focus the image, coarse focusing knob is first used and then the fine focusing knob is adjusted to get the clear image. The revolving nosepiece consists of different objectives. This can rotated to change the magnification of the microscope. Each objectives has the lens of different magnification. The microscope magnification can be determined by multiplying the objective lens value to the eyepieces lens value (which is 10X). For example, if a 10X objective is used then the total magnification is 100X. This optical microscope used in this study was capable to provide magnification up to 1000X. To view samples at higher magnification typically electrons microscopes are used. In addition to the standard bright light microscopy, polarized light microscopy technique was available with this microscope. It is a technique which uses polarized light to illuminate the sample. The direct light from the light source is blocked by two polarizer oriented from each other. The captured dual-polarized image gives details about the crystal orientation and grain structure of the Sn in the solder alloys. The desired image is captured and analyzed using the Image Pro Plus software.

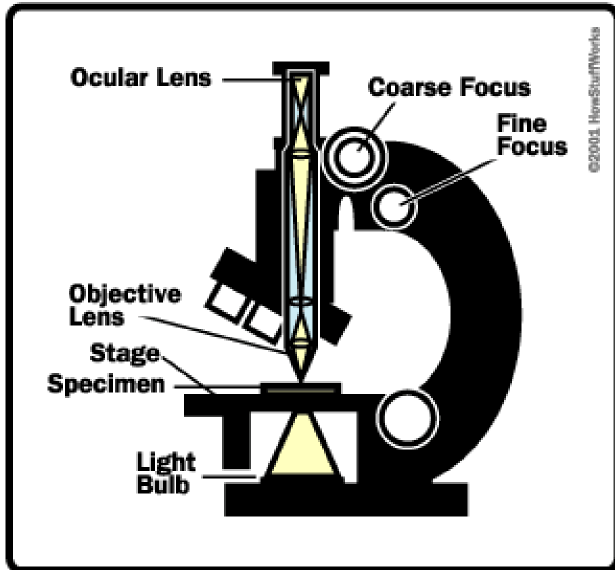

Figure 10 - Working Principle of Optical Microscope

2.13 Scanning Electron Microscope (SEM) Analysis

The microstructural analysis was performed on the cross-sectioned samples using scanning electron microscope (SEM) in order to study the size and distribution of various precipitates in the solder substrate interface and in the bulk solder. The Scanning Electron Microscope (SEM) uses a beam of electrons to form an image. SEM focuses a high-energy beam of electrons on the surface of the specimen and the signal from electron-sample gives details about solder morphology.

The main components for the working principle of SEM are vacuum chamber, electron gun, electromagnetic lenses, anode, X-ray detector, secondary electron detector, backscatter detector and specimen stage. The Figure 11 illustrates the various components of a scanning electron microscope [49]. Electron gun and various focusing lenses transmit the beam of electrons down to the specimen in the chamber. These electromagnetic lenses focus the electron beam to the specimen.

The electrons are accelerated through the focusing tube, by having an anode at the base of the electron gun. Since the anode is positively charged, the negatively charged electrons are

attracted. There is a hole in the middle of the anode, so the electron beam will pass through. The specimen stage at the bottom where the sample is placed is also positively charged, so this also keeps the electron beam moving in that direction. When the electron bean hits the specimen, two types of electrons are produced: a) secondary electrons and b) back scattered electrons.

Secondary Electrons -When electron beam hits the atoms of the specimen, those atoms absorb the energy and give off the electrons which are called as secondary electrons. There is a secondary electron detector, which has positively charged particles in it. This detects these electrons and the detector uses the information from this electron to form the image on the screen. Secondary electrons are surface electrons and they are good for getting surface features.

Backscattered electrons - These electrons do not come off the atoms like the secondary electrons. When the incident electron beam collides with nucleus of the sample atom, it reflects back out of the sample as a backscattered electron. Backscattered electrons are reflected electrons that come from deeper in from the specimen. Backscattered electrons have higher energies than the secondary electrons because the sample with higher density creates more of them which are used to form backscattered electron image.

X-ray radiation is also generated during the operation of scanning electron microscope which is characteristic for the chemical element present in the sample. If the energy and the intensity of the x-ray radiation can be measured with the x-ray detector then the elemental composition of the sample can be determined. The SEM is also equipped with an energy dispersive spectroscopy (EDS) detector. EDS analysis is carried out to determine different elements present on the sample microstructure. The EDS micrograph tells the elements present. The Y-axis tells the counts (i.e)

number of x-rays received and detected by the detector in the operational window and the X-axis represents energy level of those counts from which the element present is identified.

The main elements for operating a scanning electron microscope are column for the electron beam generation, specimen chamber, vacuum pump, control panels and monitor. First, the vacuum pump control is turned on and this vents the specimen chamber. After equalizing the pressure in the specimen chamber the cover plate is opened. To prepare the specimen a few steps need to be followed. The cross-sectioned specimen is coated with the gold palladium using a sputter coater, as non-conducting materials are subject to charging under electron beam imaging. By keeping it in the vacuum chamber it removes moisture present in the specimen, oil and other dirt. The prepared sample is then loaded into the specimen chamber and the cover plate is closed. Now the high vacuum pump is turned on and the electronic control is started. It takes some time to achieve sufficient vacuum in the chamber. Then, the motorized stage is initialized and the microscope scope controller is started. The accelerated voltage is adjusted until the reasonable image is obtained. The working accelerated voltage can range from 2 to 40kv; however 15kv is a good starting point.

SEM analysis was performed for the after reflow and aged conditions. From SEM/EDS analysis the solder joint microstructures, the intermetallic compounds formed and its composition were examined. Elemental mapping was also used for this study.

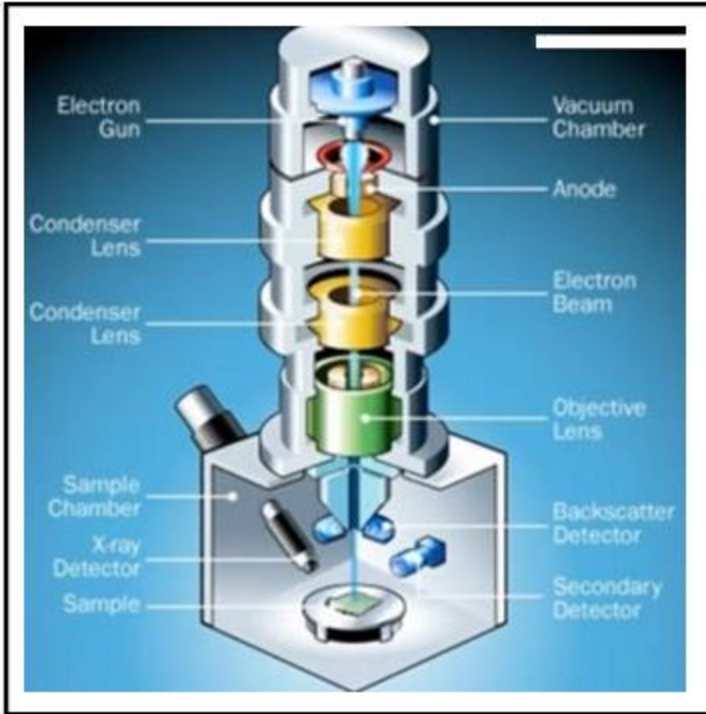

Figure 11 - Working Principle of Scanning Electron Microscope

2.14 IMC Growth Evaluation

ImageJ software was used in evaluating the thickness of IMC growth. First, the scale is set with respect to the scale in the image selected. Then, vertical lines are drawn based on the IMC growth. The imageJ software provides the length of the vertical lines with respect to the set scale. The measured set of length is averaged to find the thickness of IMC growth. The Figure 12 below shows a sample IMC thickness measurement. The yellow lines are vertical lines and measured length is then averaged to find the IMC thickness.

Figure 12 - IMC Growth Thickness Measurement

3.0 Chapter 3 - Results and Discussion

In this section the shear strength analysis, failure analysis and microstructural evaluation are discussed for various mixed solder alloy combinations that are used in two different reflow profiles (low temperature and high temperature). As discussed earlier, fifteen solder bumps were sheared for each combination and the shear forces are noted.

A) Sn99CN Process

In this study, SnBi solder pastes L20, L23, L27 mixed Sn99CN solder ball is called as Sn99CN process. The solder alloy composition, size of solder ball and the reflow profile with peak temperature in Sn99CN process are restated in Table 10 below.

Paste / Composition wt%	Solder Ball (size) / Composition wt%	Reflow Profile (Peak Temp °C)
L20 = Sn/58Bi	Sn99CN(18mils) Sn/1.1Ag/0.7Cu/0.05Ni+α	Low Temperature Reflow Profile (177°C)
L23 = Sn/57Bi/1Ag		
L27 = Sn/40Bi-Cu-Ni		
L20 = Sn/58Bi		High Temperature Reflow Profile (217°C)
L23 = Sn/57Bi/1Ag		
L27 = Sn/40Bi-Cu-Ni		

Table 10 - Sn99Cn Process

After reflow condition

Shear test is carried out for the Sn99CN process and the shear test parameters are shown in table 8 in the experimental approach section (chapter 2). Looking into the shear force for the after reflow condition, the mean value of the shear strength of L20+Sn99CN in low temperature reflow profile and high temperature reflow profile is 65.54MPa and 81.35MPa respectively. A 2-sample t-test with 95% confidence interval was carried out and from the statistical analysis a significant change in the shear strength between the low temperature reflow profile and high temperature reflow profile was observed. For L23+Sn99CN case in the low temperature reflow profile and high temperature reflow profile, the shear strength is 76.39MPa and 91.72MPa respectively. In this case, for the 2-sample t-test with 95% confidence interval, there is a significant change in the shear strength between the low temperature reflow profile and high temperature reflow profile. For L27+Sn99CN case in low temperature reflow profile and high temperature reflow profile, the shear strength is 68.13MPa and 74.74MPa. For the 2 sample t-test with 95% confidence interval, there is no significant effect in the shear strength between the low temperature reflow profile and high temperature reflow profile. Figure

13 shows the Box plot containing shear strength of Sn99CN process in as-soldered condition. From the box plot analysis it can be clearly seen that the shear strength of the high temperature reflow process is higher than low temperature reflow process in all the paste-ball combinations.

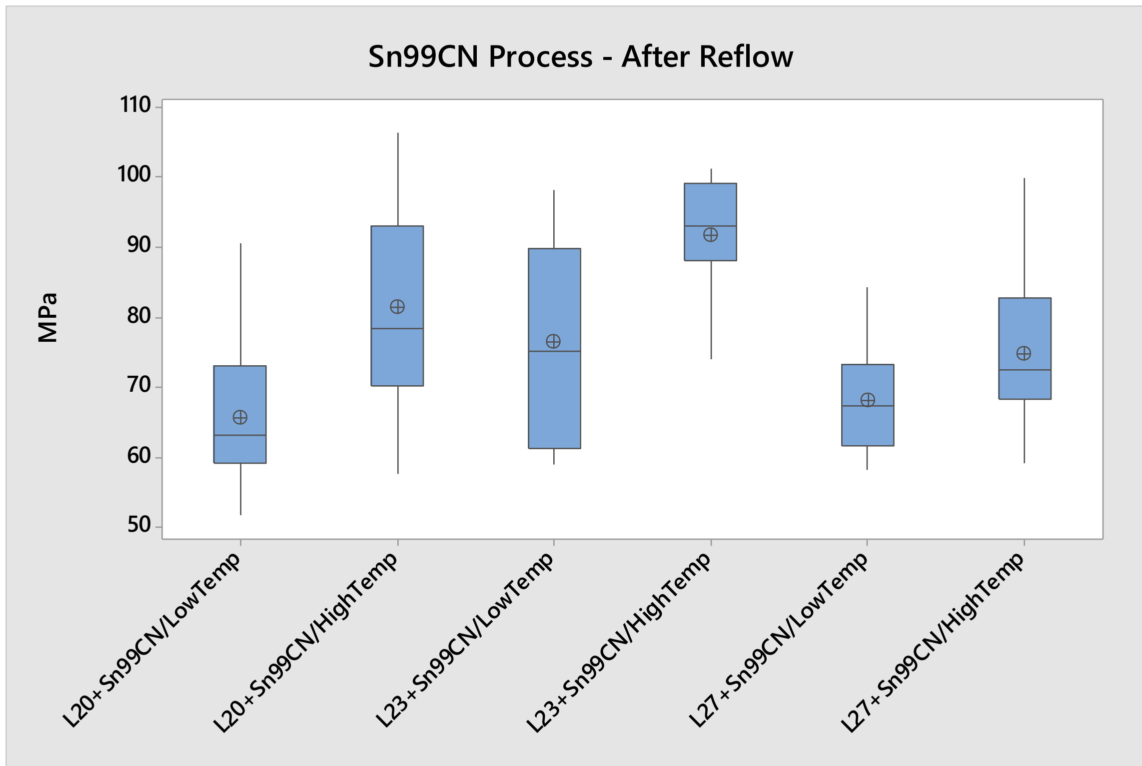

Figure 13 - Box plot containing shear strength of Sn99CN process in after reflow condition

After aging condition

After the aging condition (125°C for 200 hours), the mean value of the shear strength of L20+Sn99CN in low temperature reflow profile and high temperature reflow profile is 73.43MPa and 100.30MPa respectively. The mean value of shear strength of L23+Sn99CN in low temperature reflow profile and high temperature reflow profile is 70.48MPa and 101.70MPa respectively. The mean value of shear strength for L27+Sn99CN in low temperature reflow profile and high temperature reflow profile is 66.29MPa and 96.51MPa. In the after aging condition, for the 2 sample t-test with 95%

confidence interval, there is a significant change in the shear strength between the low temperature reflow profile and high temperature reflow profile for all the three paste-ball combinations.

Overall for the Sn99CN process (1.1 wt% Ag alloy), the L23+Sn99CN/ High temperature profile solder alloy looks to have better strength than the L20+Sn99CN and L27+Sn99CN mixed solder alloys in after reflow and after aging condition. The Figure 14 shows the Box plot containing shear strength of Sn99CN process in aged condition. The Table 11 below shows the mean shear strength comparison of S99CN process in after reflow and after aging condition.

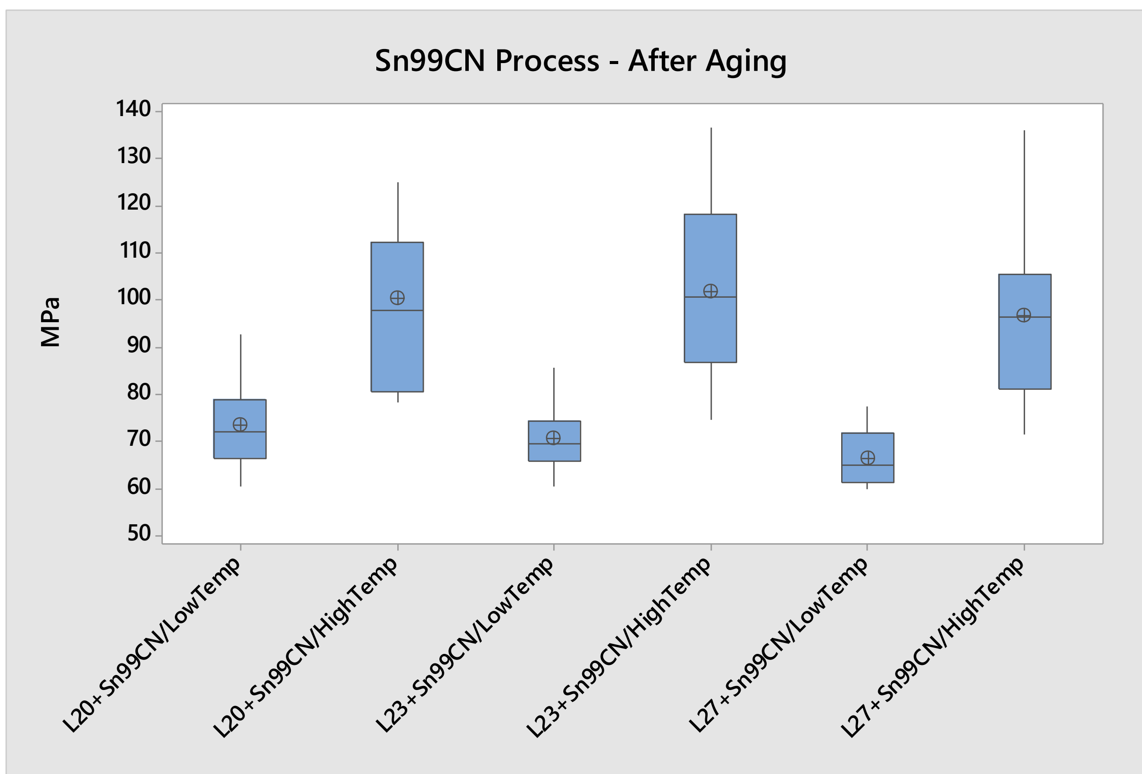

Figure 14 -Box plot containing shear strength of Sn99CN process in aged condition

Solder Sphere	Solder Paste	Reflow Profile	Mean Shear Strength in MPa (After Reflow)	Mean Shear Strength in MPa (Aging)
Sn99CN	L20	Low Temp	65.54	73.43
		High Temp	79.36	99.17
	L23	Low Temp	76.39	70.48
		High Temp	91.72	101.45
	L27	Low Temp	68.13	66.11
		High Temp	74.53	96.51

Table 11 -Mean shear strength of Sn99CN process before and after aging conditions

B) Sn100C Process

In this study, SnBi solder pastes L20, L23, L27 mixed with Sn100C solder ball is called as Sn100C process. The solder alloy composition, size of solder ball and the reflow profile with peak temperature in Sn99CN process are restated in Table 12 below.

Paste / Composition wt%	Solder Ball (size) / Composition wt%	Reflow Profile (Peak Temp °C)
L20 = Sn/58Bi	Sn100C(20mils) Sn/0.7Cu/0.05Ni+Ge	Low Temperature Reflow Profile (177°C)
L23 = Sn/57Bi/1Ag		
L27 = Sn/40Bi-Cu-Ni		
L20 = Sn/58Bi		High Temperature Reflow Profile (217°C)
L23 = Sn/57Bi/1Ag		
L27 = Sn/40Bi-Cu-Ni		

Table 12 - Sn100C process

After reflow condition

Looking into the shear force for the after reflow condition, the mean value of the shear strength of L20+Sn100C in low temperature reflow profile and high temperature reflow profile is 73.05MPa and 81.85MPa respectively. A 2-sample t-test with 95% confidence interval was carried out and from the statistical analysis a significant change in the shear strength between the low temperature reflow profile and high temperature reflow profile was observed. For L23+Sn100C case in the low temperature reflow profile and high temperature reflow profile, the shear strength is 64.48MPa and 83.07MPa respectively. In this case, for the 2 sample t-test with 95% confidence interval, there is also a significant change in the shear strength between the low temperature reflow profile and high temperature reflow profile. For L27+Sn100C case in low temperature reflow profile and high temperature reflow profile, the shear strength is 68.70MPa and 71.57MPa. For the 2 sample t-test with 95% confidence interval, there is no significant effect in the shear strength between the low temperature reflow profile and high temperature reflow profile. Figure 15 shows the Box plot containing shear strength of Sn99CN process in as-soldered condition. From the box plot analysis, it

can be clearly seen that the shear strength of the high temperature reflow process is higher than low temperature reflow process in all the paste-ball combinations.

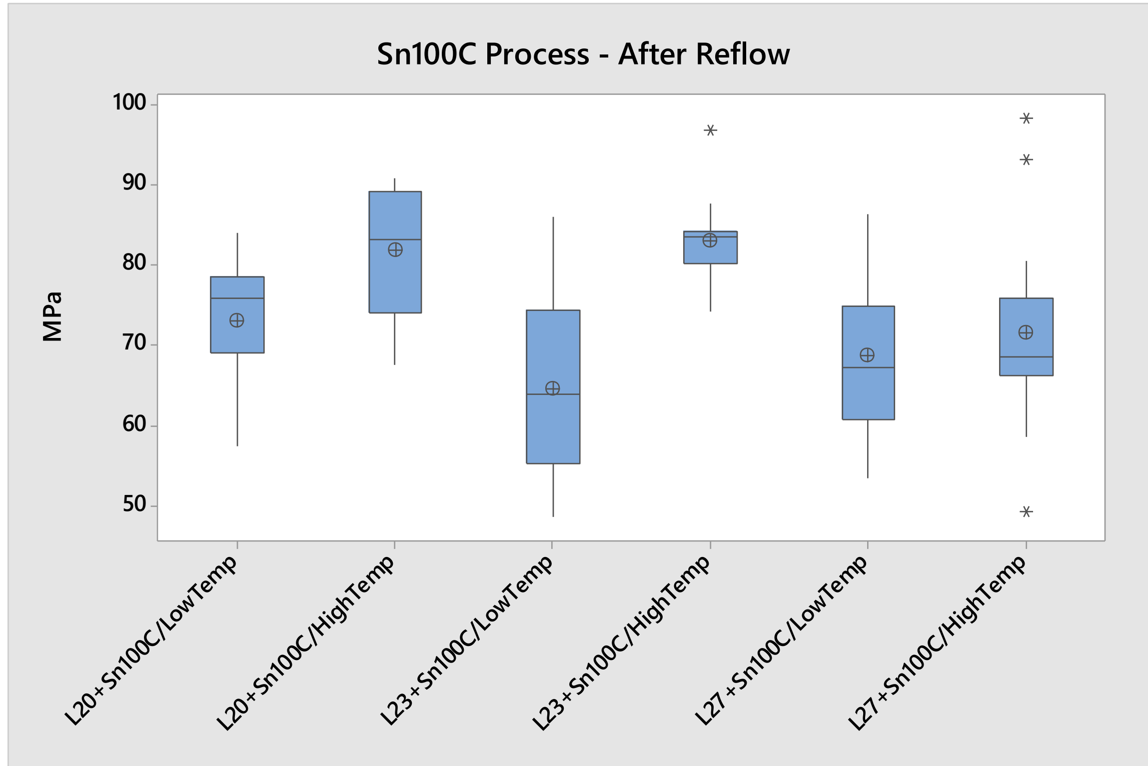

Figure 15 - Box plot containing shear strength of Sn100C process in after reflow condition

After aging condition

After the aging condition (125°C for 200 hours), the mean value of the shear strength of L20+Sn100C in low temperature reflow profile and high temperature reflow profile is 67.97MPa and 82.95MPa respectively. The mean value of shear strength of L23+ Sn100C in low temperature reflow profile and high temperature reflow profile is 67.31MPa and 85.19MPa respectively. The mean value of shear strength for L27+ Sn100C in low temperature reflow profile and high temperature reflow profile is 63.45MPa and 76.78MPa. In the after aging condition, for the 2 sample t-test with 95% confidence interval, there is a significant change in the shear strength between the

low temperature reflow profile and high temperature reflow profile for all the three paste-ball combinations.

Overall for the Sn100C process (no Ag alloy), the L23+Sn100C/ High temperature profile solder alloy looks to have better strength than the L20+Sn100C and L27+Sn100C mixed solder alloys in after reflow and after aging condition. The Figure 16 shows the Box plot containing shear strength of Sn100C process in aged condition. The Table 13 below shows the mean shear strength comparison of Sn100C process in after reflow and after aging condition.

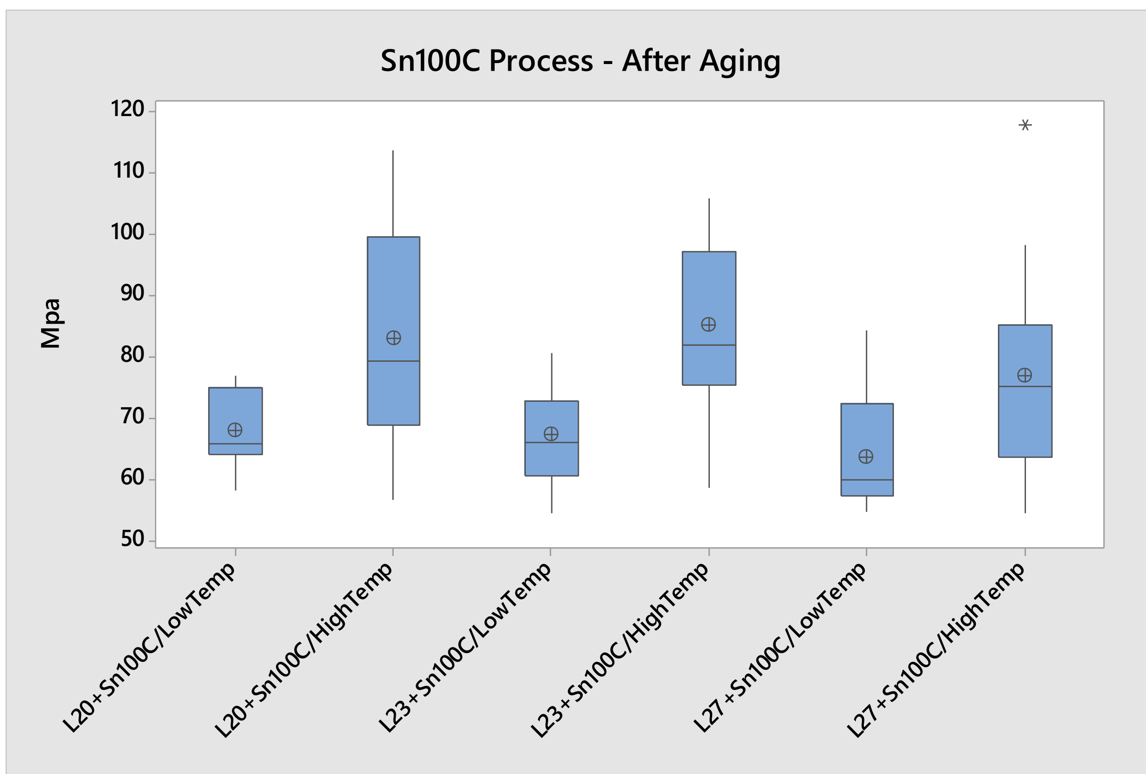

Figure 16 - Box plot containing shear strength of Sn100C process in aged condition

Solder Sphere	Solder Paste	Reflow Profile	Mean Shear Strength in MPa (After Reflow)	Mean Shear Strength in MPa (Aging)
Sn100C	L20	Low Temp	73.05	67.97
		High Temp	81.63	82.95
	L23	Low Temp	64.48	67.31
		High Temp	83.07	85.19
	L27	Low Temp	68.70	63.29
		High Temp	71.57	76.78

Table 13 - Mean shear strength of Sn100C process before and after aging conditions

C) SAC Process

In this study, SnBi solder pastes L20, L23, L27 mixed Sn100C solder ball is called as Sn100C process. The solder paste composition, solder ball composition, size of solder ball and the reflow profile with peak temperature in Sn99CN process are restated in Table 14 below.

Paste / Composition wt%	Solder Ball (size) / Composition wt%	Reflow Profile (Peak Temp ^{o}C)
L20 = Sn/58Bi	SAC305 (30mils) Sn/3.0Ag/0.5Cu	Low Temperature Reflow Profile (177°C)
L23 = Sn/57Bi/1Ag		
L27 = Sn/40Bi-Cu-Ni		
L20 = Sn/58Bi		High Temperature Reflow Profile (217°C)
L23 = Sn/57Bi/1Ag		
L27 = Sn/40Bi-Cu-Ni		

Table 14 - SAC305 process

After reflow condition

Looking into the shear force for the after reflow condition, the mean value of the shear strength of L20+SAC305 in low temperature reflow profile and high temperature reflow profile is 40.05MPa and 68.32MPa respectively. A 2-sample t-test with 95% confidence interval was carried out and from the statistical analysis a significant change in the shear strength between the low temperature reflow profile and high temperature reflow profile was observed. For L23+ SAC305 case, in the low temperature reflow profile and high temperature reflow profile, the shear strength is 46.65MPa and 86.09MPa respectively. In this case, for the 2-sample t-test with 95% confidence interval, there is also a significant change in the shear strength between the low temperature reflow profile and high temperature reflow profile. For L27+ SAC305 case, in low temperature reflow profile and high temperature reflow profile, the shear strength is 48.86MPa and 81.87MPa. For the 2-sample t-test with 95% confidence interval, there is significant change in the shear strength between the low temperature reflow profile and high temperature reflow profile. Figure 17 shows the Box plot containing shear strength of SAC305 process in as-soldered condition. From the box plot analysis it can be clearly seen that the shear strength of the high temperature reflow process is higher than low temperature reflow process in all the paste-ball combinations.

Overall for the SAC305 process (3wt% Ag alloy), the L23+SAC305/High temperature profile solder alloy looks to have better strength than L20+SAC305 and L27+SAC305 mixed solder alloys. The reason for L23 paste with lead-free solder alloys having higher shear strength than the other mixed solder alloys is the presence of silver in the L23 paste. With 1% silver in the L23 SnBi paste, it reduces the melting temperature of the solder alloy, improves wetting and gives better mechanical strength.

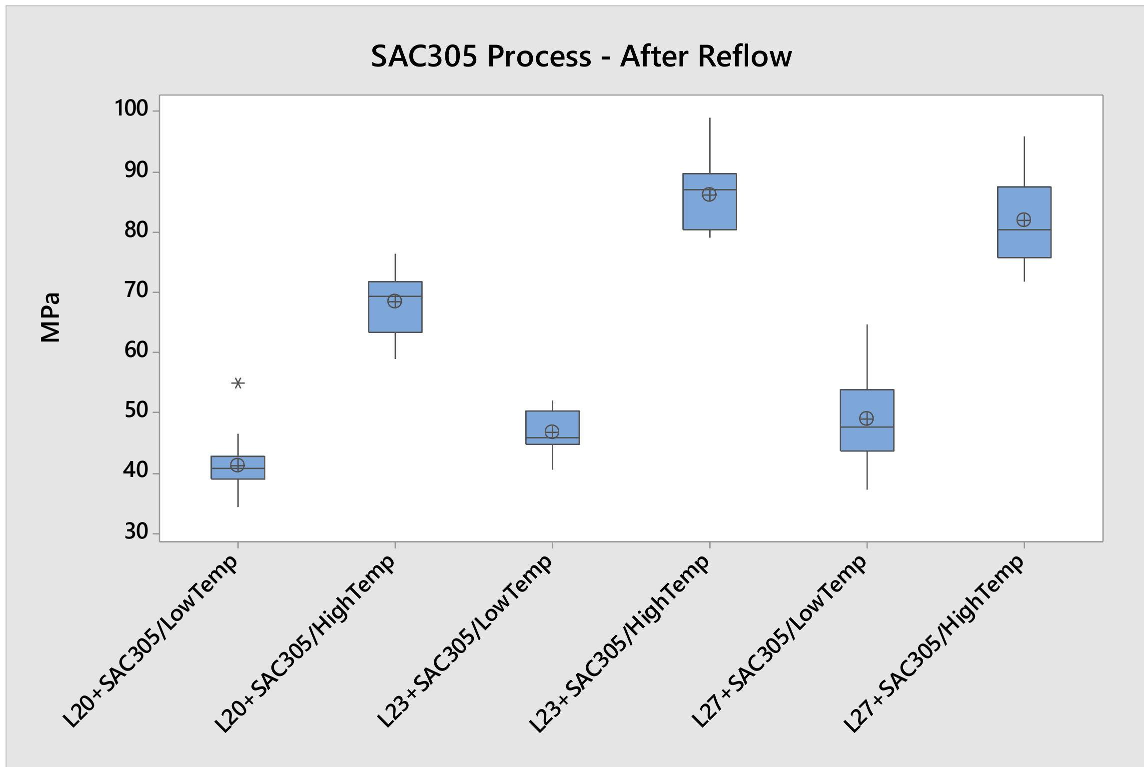

Figure 17 - Box plot containing shear strength of SAC305 process in after reflow

After aging condition

After the aging condition (125°C for 200 hours), the mean value of the shear strength of L20+SAC305 in low temperature reflow profile and high temperature reflow profile is 45.83MPa and 64.58MPa respectively. The mean value of shear strength of L23+SAC305 in low temperature reflow profile and high temperature reflow profile is 40.30MPa and 75.82MPa respectively. The mean value of shear strength for L27+SAC305 in low temperature reflow profile and high temperature reflow profile is 35.02MPa and 80.45MPa respectively. In the after aging condition, for the 2 sample t-test with 95% confidence interval, there is a significant change in the shear strength between the low temperature reflow profile and high temperature reflow profile for all the three paste-ball combinations. Figure 18 shows the Box plot containing shear strength of SAC305 process

in after aging condition. The Table 15 below shows the mean shear strength comparison of Sn100C process in after reflow and after aging condition.

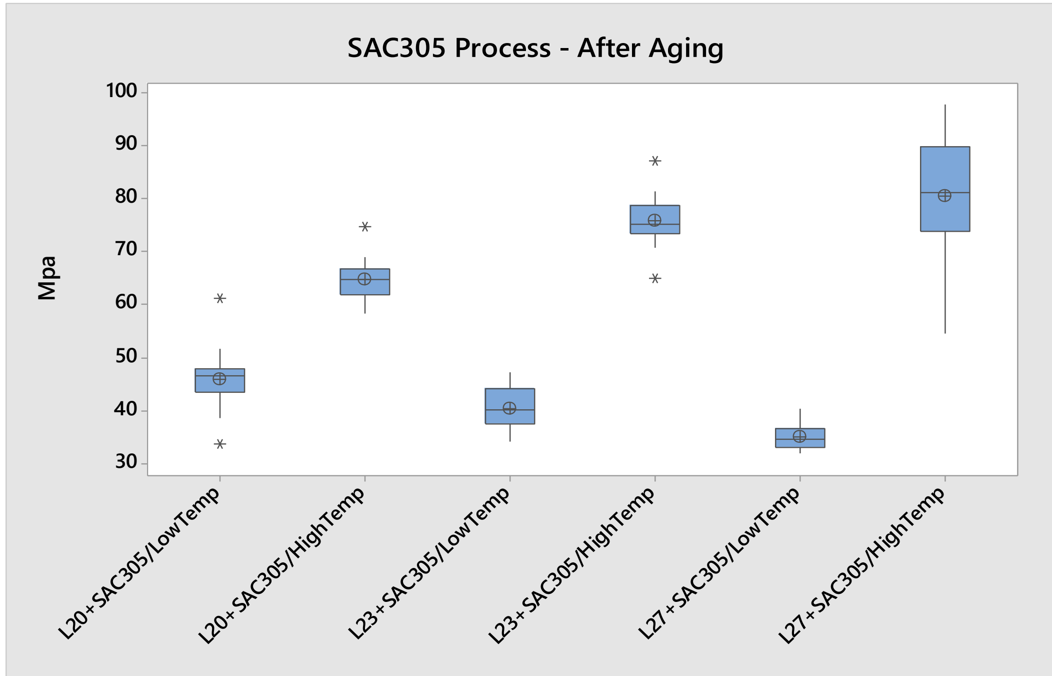

Figure 18 - Box plot containing shear strength of SAC305 process in aged condition

Solder Sphere	Solder Paste	Reflow Profile	Mean Shear Strength in MPa (After Reflow)	Mean Shear Strength in MPa (Aging)
SAC305	L20	Low Temp	40.05	45.83
		High Temp	68.19	65.22
	L23	Low Temp	46.65	40.30
		High Temp	86.09	75.82
	L27	Low Temp	48.86	35.01
		High Temp	81.87	79.87

Table 15 - Mean shear strength of SAC305 process before and after aging conditions

Comparing the shear strength between the after reflow condition and the aged conditions, there is not much of a trend. The mean shear strength is almost same in some of the cases or it varies by a small margin in some cases which can be seen in the table above. A paired t test statistical analysis with 95% confidence interval was carried out in comparing the shear strength of the after reflow and after aging conditions. The following paste-ball combinations were found to have no effect on those two conditions: L23+Sn99CN/LowTemp, L27+Sn99CN/HighTemp, L20+Sn100C/HighTemp,L23+Sn100C/LowTemp,L23+Sn100C/HighTemp,L27+Sn100C/HighTemp and L27+SAC305/HighTemp. Rest of the combinations was found to be statically significant.

From the shear strength analysis, it can be seen that in all the three processes the shear strength of high temperature reflow profile is higher than the low temperature reflow profile. Moreover, the statistical analysis clearly shows that there is a significant change in the shear strength of high temperature reflow profile and low temperature reflow profile, which is consistent with all the solder ball-paste combinations. The reason for the higher shear strength in the high temperature reflow profile is improved mixing and smaller Bi precipitates which will be explained in detail in the failure analysis part. The improved mixing in high temperature reflow process is because of the peak temperature of high temperature reflow profile which is 217℃ whereas the peak temperature of low temperature reflow profile is 177℃. With the higher peak temperature in high temperature process, the lead-free solder balls are able to melt and coalesce well with the SnBi paste which is the reason for higher shear strength in high temperature reflow process.

3.1 Failure Analysis

The master polished cross section samples were evaluated using the optical microscopes to study the solubility of SnBi paste on lead-free solder balls. First, SnBi paste with SAC ball is evaluated. For the low temperature reflow profile there was not much of a dissolution in the mixed

solder alloy combinations which can be seen in Figure 19a where the paste on the bottom and the ball on the top can be seen clearly. Whereas with the high temperature reflow profile, the tin has completely dissolved into the bismuth as shown in Figure 19b where the ball and paste are completely dissolved. This change in the dissolution is because of the difference in the peak temperature of the two reflow profiles. With the low temperature reflow profile the SAC ball is not able to melt completely as its melting temperature is 215°C and peak temperature of the reflow profile is 177°C. However, in the high temperature reflow profile, with the peak reflow temperature of 217°C the bismuth paste and SAC305 balls are able to dissolve better than the low temperature reflow profile. For the SAC305 process, with L20, L23 and L27 pastes for the low temperature reflow profile the solubility of tin in bismuth is very small. Whereas for the high temperature reflow profile the SnBi paste is completely dissolved. The Figure 20 below shows the cross-polarized images of L20+SAC305. The Figure 20a shows the cross-sectioned image of low temperature profile which has interlaced and beach ball structure whereas Figure 20b represents High temperature profile which has single grain structure. Unlike single grain structure, many small boundaries are present in interlaced structure.

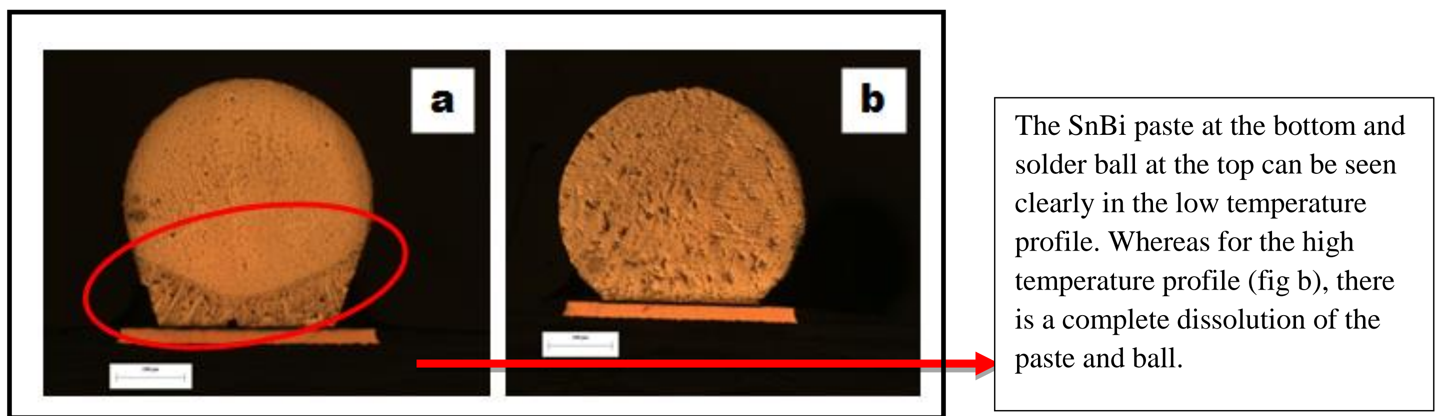

Figure 19 - Cross section of L20+SAC305 a) Low temperature reflow Profile b) High temperature reflow profile

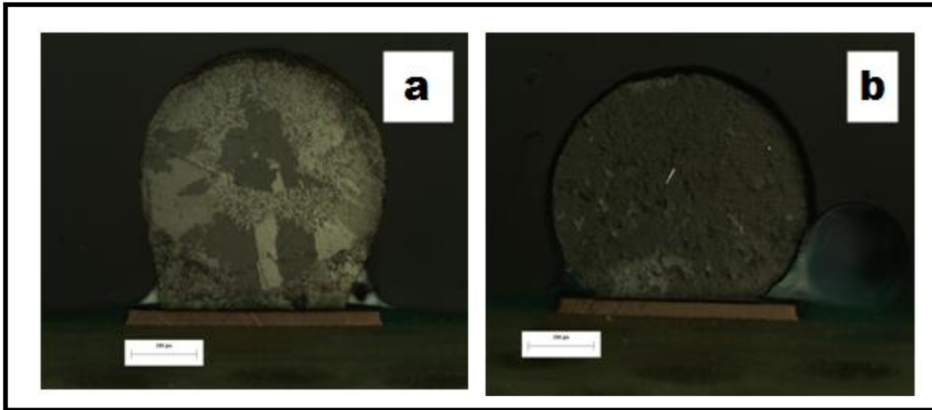

Figure 20 - Cross Polarized Image of L20+SAC305 a) Low temperature reflow Profile b) High temperature reflow profile

For the Sn100C process, with the L20, L23 and L27 pastes for the low temperature reflow profile there is no dissolution between SnBi paste and the Sn100C ball(Figure 21a) which is same as the SAC305 process, whereas for the high temperature reflow profile the SnBi is partially dissolved with Sn100C solder ball which can be seen in Figure 21b. The partial dissolution in Sn100C process may be because of very high melting temperature of Sn100C ball which is 227°C. Therefore, at a peak reflow temperature of 217°C the Sn100C ball is not able to dissolve completely as it did for SAC305 ball. The Figure 22 below shows the cross-polarized images of L23+Sn100C. The Figure 22a shows the cross polarized image of low temperature profile which has single grain structure whereas Figure 22b represents high temperature profile which has interlaced structure.

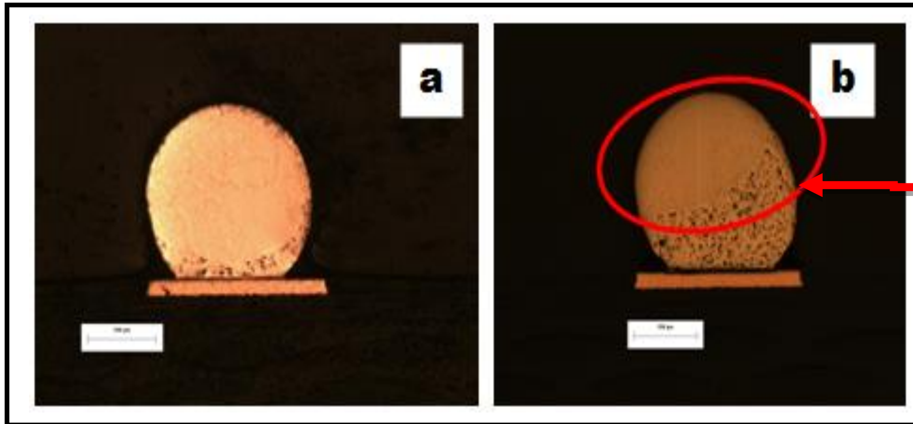

Figure 21 - Cross section of L23+Sn100C a) Low temperature reflow Profile b) High temperature reflow profile

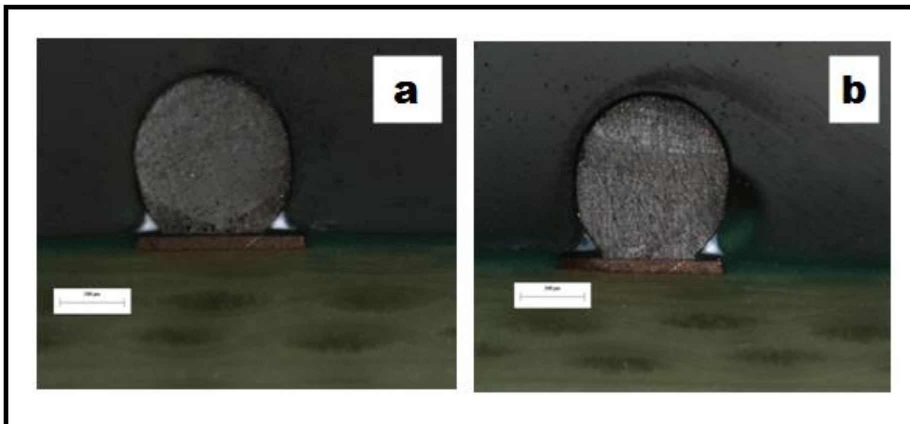

Figure 22 -Cross Polarized Image of L23+Sn100C a) Low temperature reflow Profile b) High temperature reflow profile

For the Sn99CN process, with L20, L23 and L27 pastes for the low temperature reflow profile, there is no dissolution between SnBi paste and the Sn99CN ball. This is consistent with all the three processes for low temperature profile. With the high temperature reflow profile L20+Sn99CN case looks almost completely (90%) dissolved. The reason for not complete dissolution is due to the high melting point of Sn99CN (227°C). With L23+Sn99CN and L27+Sn99CN/High temperature profile, tin has completely dissolved into the SnBi paste which can be seen in Figure 23.

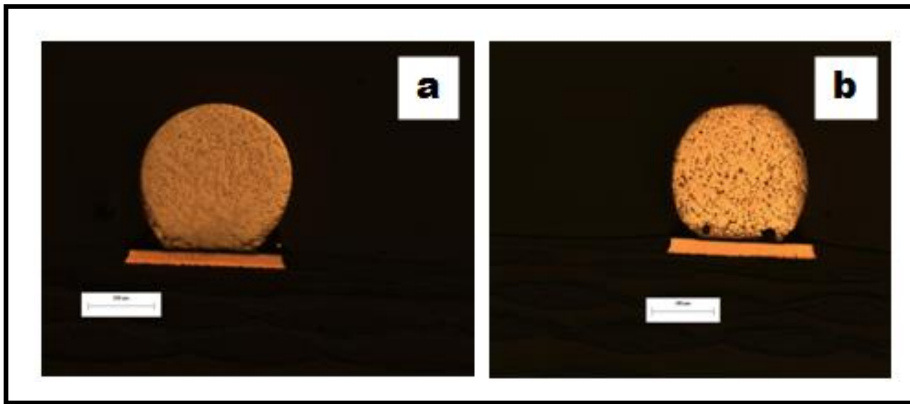

Figure 23 - Cross section of L27+Sn99CN a) Low temperature reflow Profile b) High temperature reflow profile

The Figure 24a below shows the cross-polarized images of L27+Sn99CN. The figure 23a shows the cross section image of low temperature profile which has beach ball structure whereas Figure 24b represents high temperature reflow profile which also has beach ball structure. The beach ball structure has three different unique Sn morphologies in it.

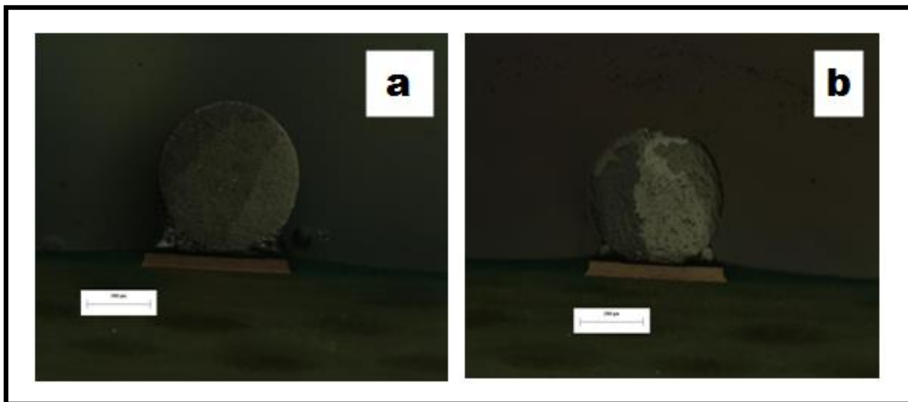

Figure 24 - Cross Polarized Image of L27+Sn99CN a) Low temperature reflow Profile b) High temperature reflow profile

From this analysis, Sn100C process looks to different from the other two process (SAC305 and Sn99CN) in terms of high temperature profile. The reason for the partial dissolution in the Sn100C process is due to the absence of silver content in the solder ball. With SAC305 and Sn99CN there are 3% and 1.1% of silver in the solder ball respectively. Therefore, with the silver content in the solder

ball, the tin is able to dissolve well in SnBi paste. Moreover, the pasty range of L23 paste is 75ºC whereas L20 is eutectic and L27 it is 30ºC. With the higher pasty range, the tin is not able to completely dissolve into the paste and hence we have the partial dissolution. So, the higher pasty range tend to affect the dissolution of the L23+Sn100C process. From this evaluation, it is evident that the Ag content in the solder ball and SnBi pasty range tends to affect the dissolution of the paste and ball.

When comparing the after aging condition, the cross section images looks to project the same kind of result (in terms of dissolution) as it did for the after reflow condition in all the three processes. The Table 16 below shows the level of solubility (partial mixed or fully mixed) and the kind of cross-polarized grain structure of various solder paste-ball combinations.

Solder Paste	Solder Sphere Alloy	Sphere Diameter	Bi wt%	Ag wt%	Peak Temp of Reflow Profile	Fully Mixed	Partially Mixed	Grain Structure
L20	SAC305	30 mils	3.56%	2.81%	177°C			BB/IL
L20	SAC305	30 mils			217°C	X		SG
L20	Sn100C	20 mils	3.53%	-	177°C			BB
L20	Sn100C	20 mils			217°C		X	IL
L20	Sn99CN	18 mils	3.73%	1.01%	177°C			BB
L20	Sn99CN	18 mils			217°C		X	SG
L23	SAC305	30 mils	3.50%	2.87%	177°C			BB/IL
L23	SAC305	30 mils			217°C	X		BB/IL
L23	Sn100C	20 mils	4.0%	0.07%	177°C			SG
L23	Sn100C	20 mils			217°C		X	IL
L23	Sn99CN	18 mils	3.71%	1.08%	177°C			BB/IL
L23	Sn99CN	18 mils			217°C	X		SG
L27	SAC305	30 mils	2.33%	2.82%	177°C			BB/IL
L27	SAC305	30 mils			217°C	X		BB
L27	Sn100C	20 mils	2.31%	-	177°C			IL/SG
L27	Sn100C	20 mils			217°C		X	BB
L27	Sn99CN	18 mils	2.46%	1.02%	177°C			BB/SG
L27	Sn99CN	18 mils			217°C	X		BB

Table 16 -Microstructure Evaluation

BB -Beach Ball

SH - Single Grain

IL - Interlaced

A representative set of cross-sections of the SnBi paste and lead-free solder balls are taken into consideration for SEM analysis to further investigate the size and distribution of various precipitates in the solder joint and in the bulk solder.

First, L27+SAC305/low temperature reflow profile, aged at 125°C for 200 hours is investigated.

Figure 25 shows the low magnification image of L27+SAC305/ low temperature profile/Aged where the paste at the bottom and the ball at the top can be seen clearly. The microstrucure of the sheared pad surface of this sample shows that there are high concentrations of bismuth in the sheared surface which can be seen in the EDS micrograph. The crack surface is 100% bismuth which evident from the EDS micrograph in Figure 29. With the low temperature process, the bismuth platelets can be seen clearly in Figure 26. This is because at low temperature profile there is no proper dissolution of SnBi paste and the ball, so the SnBi paste with high concentration of bismuth remains on the pad surface. A cross section was prepared following shear testing to further inspect the crack propagation path. It can be seen clearly that the crack is propagating transgranularly along the weak Bi rich phase near the Cu pad intermetallic which can be seen in Figure 27. There is no tin in the crack surface because there is more bismuth phase near the tin copper interface which gives a continuous interface for cracks to propagate which can seen in Figure 27. As a result of high concentration of bismuth in the pad surface, all of the failure modes for the low temperature reflow process are brittle defects which can be seen in Figure 28 as bismuth is said to have brittle mechanical property.

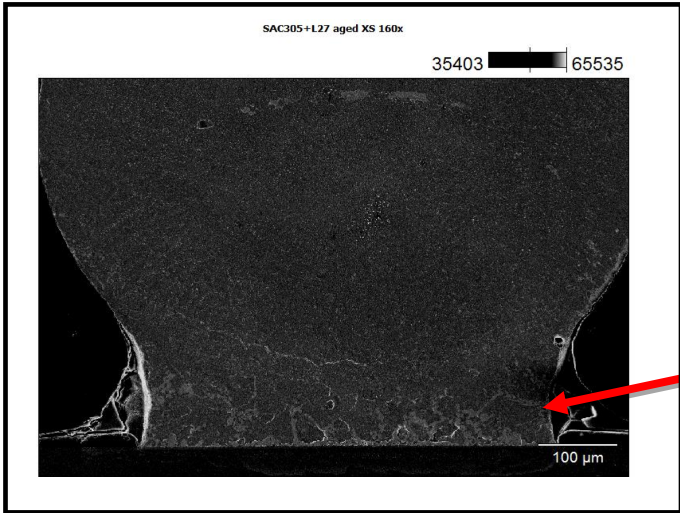

Figure 25 - Low Magnification Image of L27+SAC305/Low Temp Profile/Aged

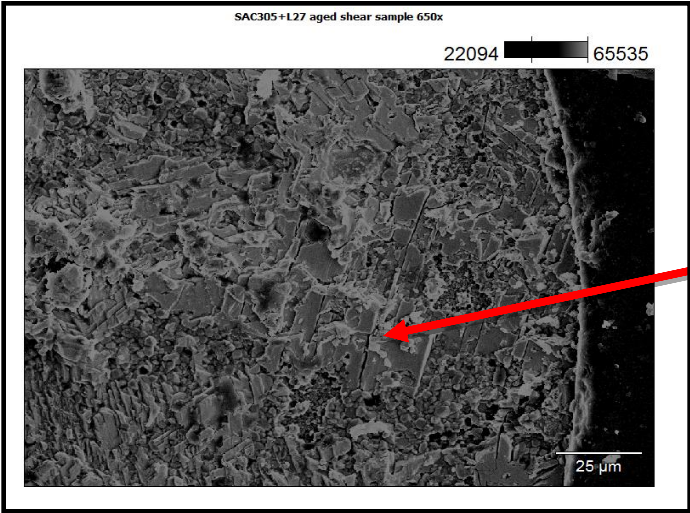

Figure 26 - Sheared Surface of L27+SAC305/Low Temp Profile/Aged

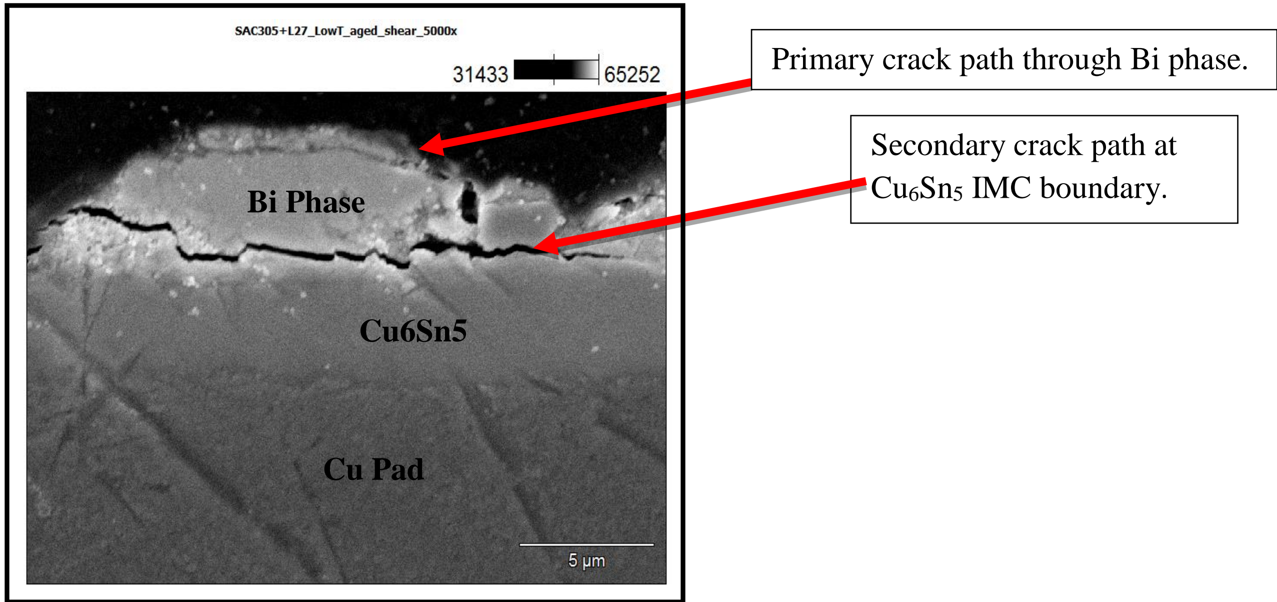

Figure 27 - Crack Propagation post Shear Test of L27+SAC305/Low Temp profile/Aged

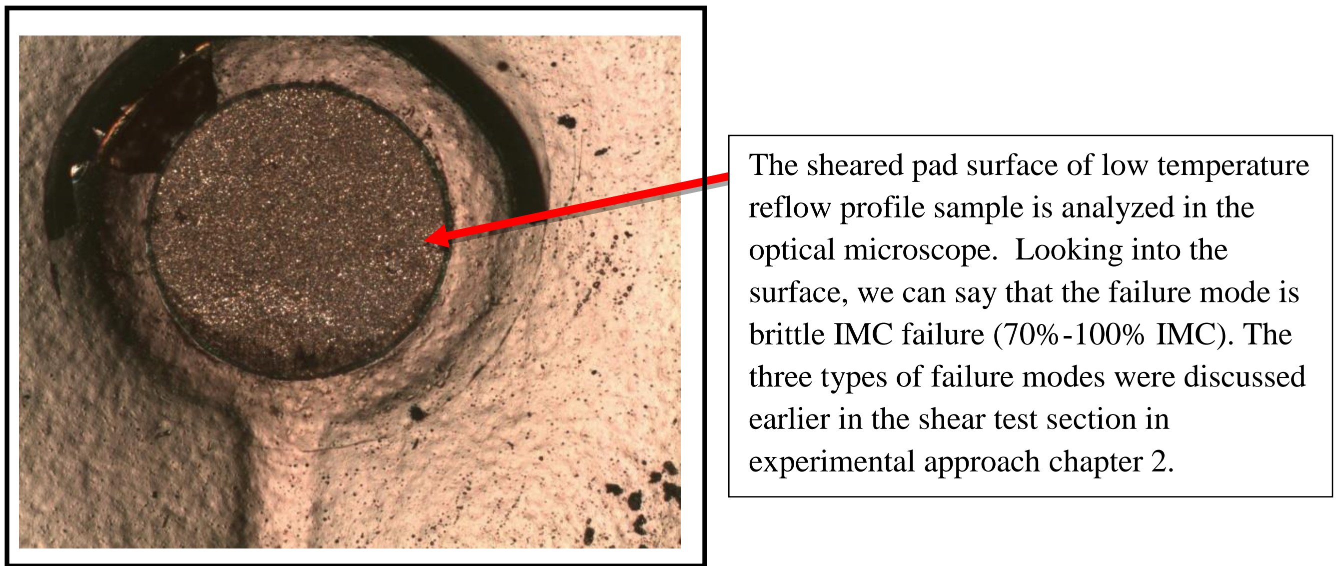

Figure 28 - L20+SAC305/Low Temp profile - Brittle Failure Mode

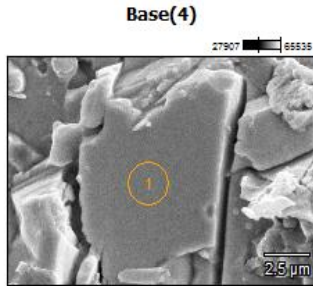

Image Name: Base(4)
Image Resolution: 1024 by 720
Image Pixel Size: 0.02 μm
Acc. Voltage: 15.0 kV
Magnification: 7000

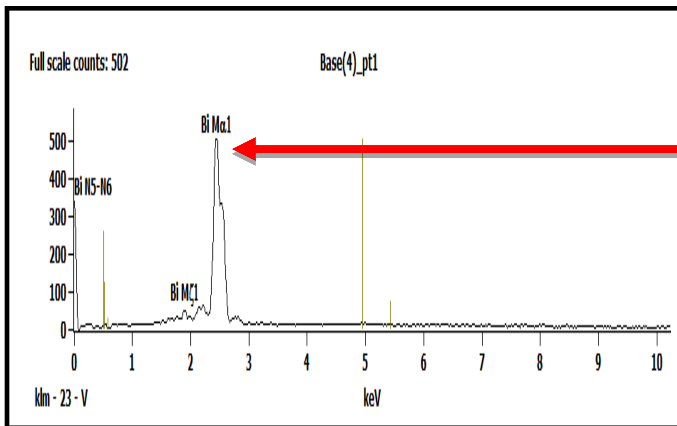

From the EDS micrograph of the sheared pad surface, high concentration of bismuth on the pad surface is evident.

Figure 29 - EDS Analysis of L27+SAC305/Low Temp profile/Aged condition

In order to study the distribution of various elements in the solder substrate interface and in the bulk solder, elemental mapping analysis was carried out using SEM. The Figure 30 below shows the elemental mapping of L27+SAC305/low temperature reflow profile, aged at 125°C for 200 hrs. Looking into the microstructure of the cross sectioned sample, the concentration of tin, bismuth and copper are high on the board side. This is because of the surface finish (copper) and the L27 paste composition (tin and bismuth). With low temperature profile there is no proper dissolution of paste and ball, and as a result the high concentration of tin, bismuth and copper are evident.

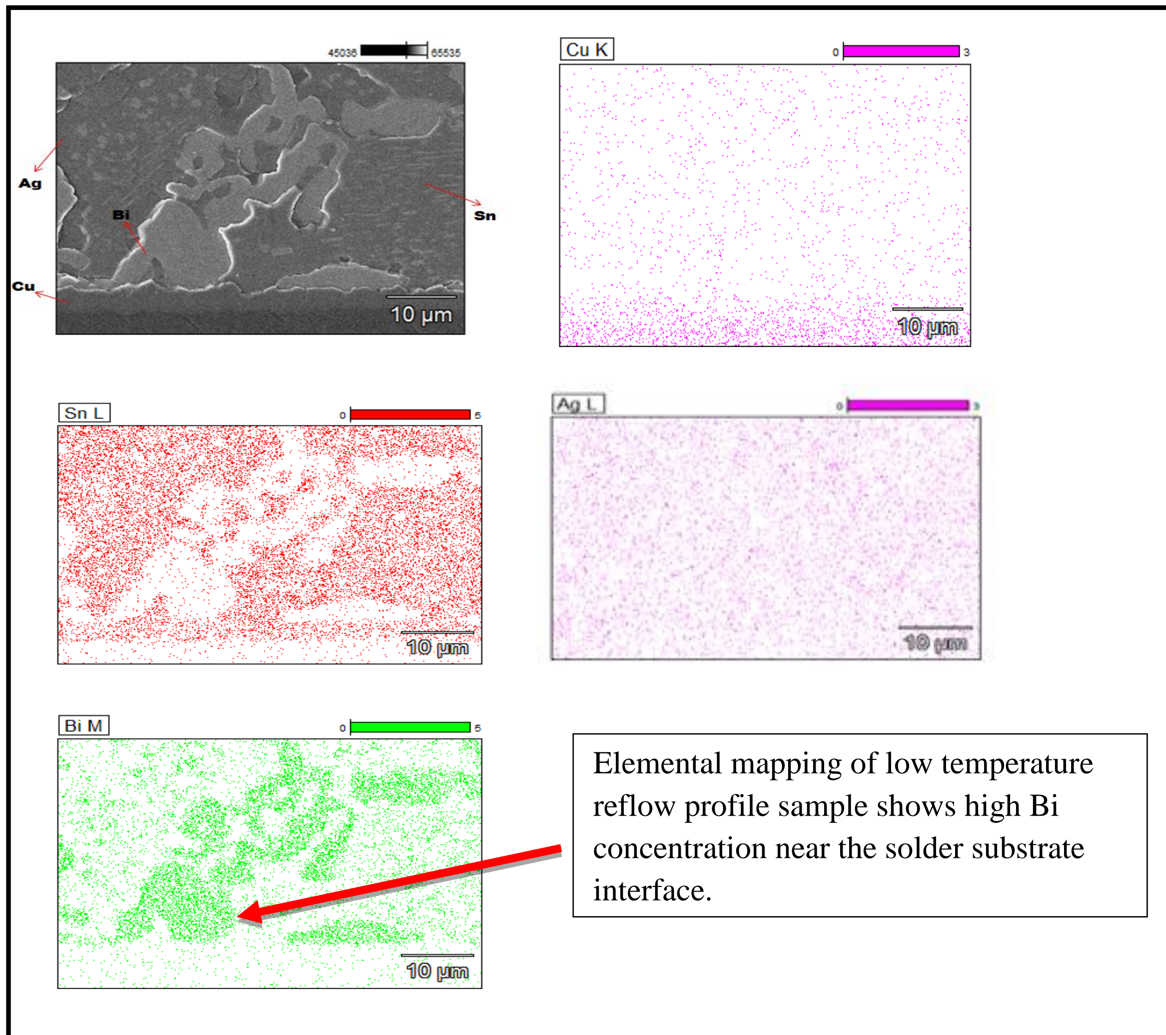

Figure 30 - Elemental Mapping of L27+SAC305/Low Temp profile/Aged

The figures shows the SEM images of L27+SAC305/High Temperature reflow profile, aged at 125°C for 200 hrs. The Figure 31a shows the low magnification image of the sample and it is evident that the SnBi paste and ball has completely dissolved. It can be seen that, with the high temperature reflow process, the concentration of bismuth on the surface of the pad is low. With peak temperature of 217°C, the SAC ball is able to dissolve well into the L27 paste. With this better coalescence, the shear strength is higher than the low temperature reflow process. Moreover, after the shear test, the fractured surfaces were examined in SEM which is shown in Figure 31a(low magnification) and Figure 32(high magnification). The sheared surface has high concentration of tin

and copper with very small percentage of bismuth. The crack propagation is in the tin copper intermetallic and Bi does not existent in the sheared surface.

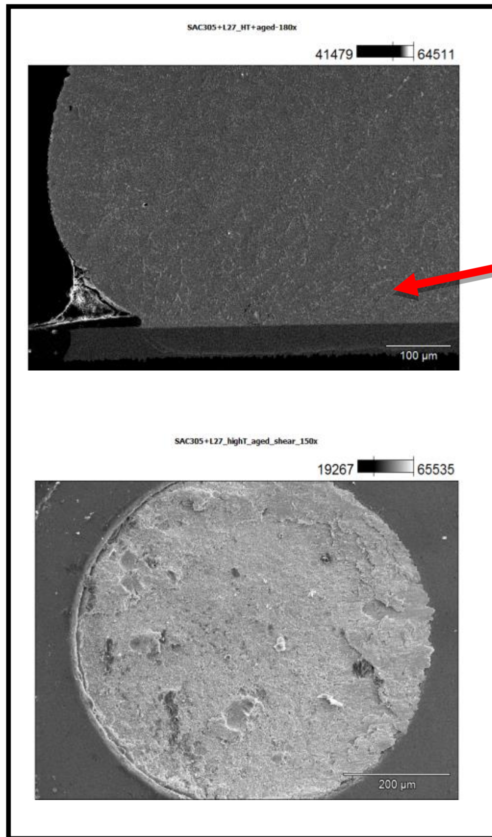

In the high temperature reflow profile, the paste at bottom and solder ball at top cannot be seen. Paste and ball are completely dissolved.

Figure 31 - a) Low Magnification Image of L27+SAC305/High Temp/Aged

b) Sheared Surface of L27+SAC305/High Temp/Aged

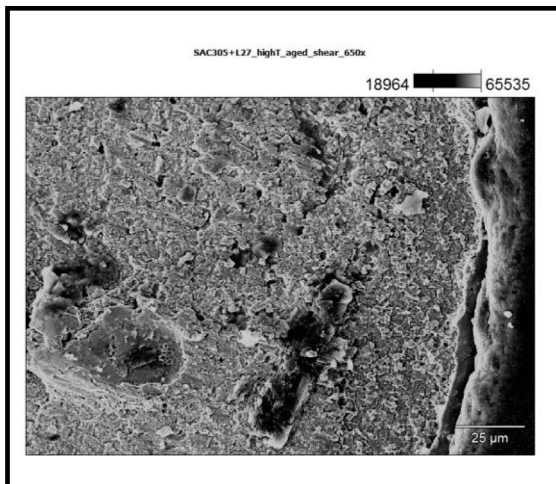

Figure 32 - Sheared Surface of L27+SAC305/High Temp profile/Aged

The Figure 33 below shows the elemental mapping of L27+SAC305/High temperature reflow profile, aged at 125°C for 200 hrs. Looking into the microstructure of the cross sectioned sample, the concentration of tin and copper are high on the board side and Bi is not present on the board side.

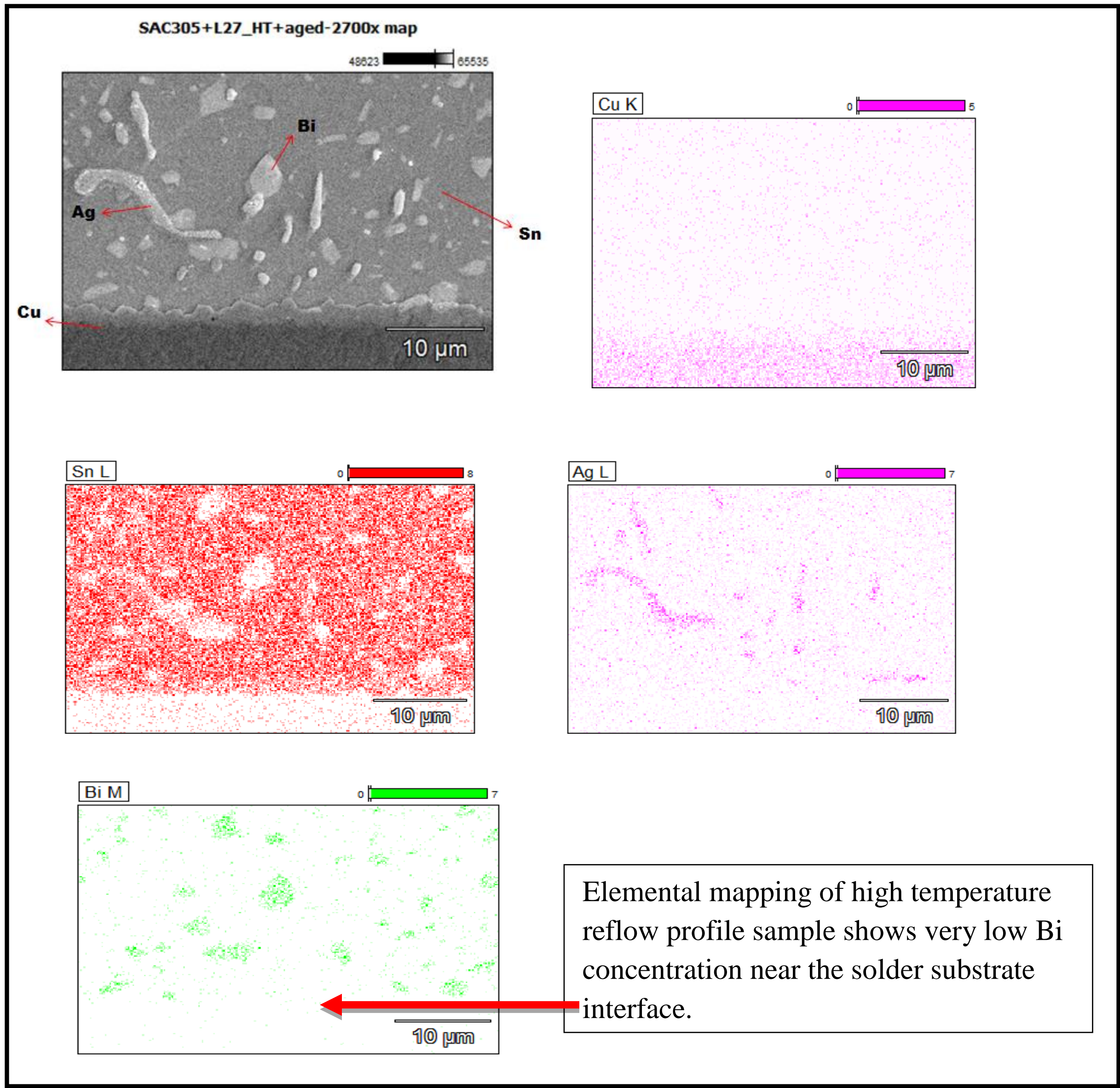

Figure 33 -Elemental Mapping of L27+SAC305/High Temp profile/Aged

Looking into the failure modes for the high temperature reflow profile process, almost 15 to 25% of the sheared surface are dual failures and rest was all brittle failures. For the SAC305 process,

40% to 60% of pad cratering defects were seen in high temperature reflow profile process. This is because, with high temperature reflow process the SAC305 balls are able to melt completely and dissolve with the SnBi paste whereas with the other two cases, the Sn100C and Sn99CN the melting temperature is 227°C so the ball does not melt to the extent as it did for SAC process. Therefore, at the high-speed shear force the crack is able to propagate through the resin material and create pad-cratering failure. The Figure 34a shows the L23+Sn99CN/High temperature profile involving dual failure (IMC+bulk Solder) and Figure 34b shows L27+SAC305/High temperature profile involving pad-cratering failure. The failures modes are almost the same in the as soldered and aged condition. The Figure 35 shows fraction of various failure mechanisms observed after the ball shear test in as-soldered condition.

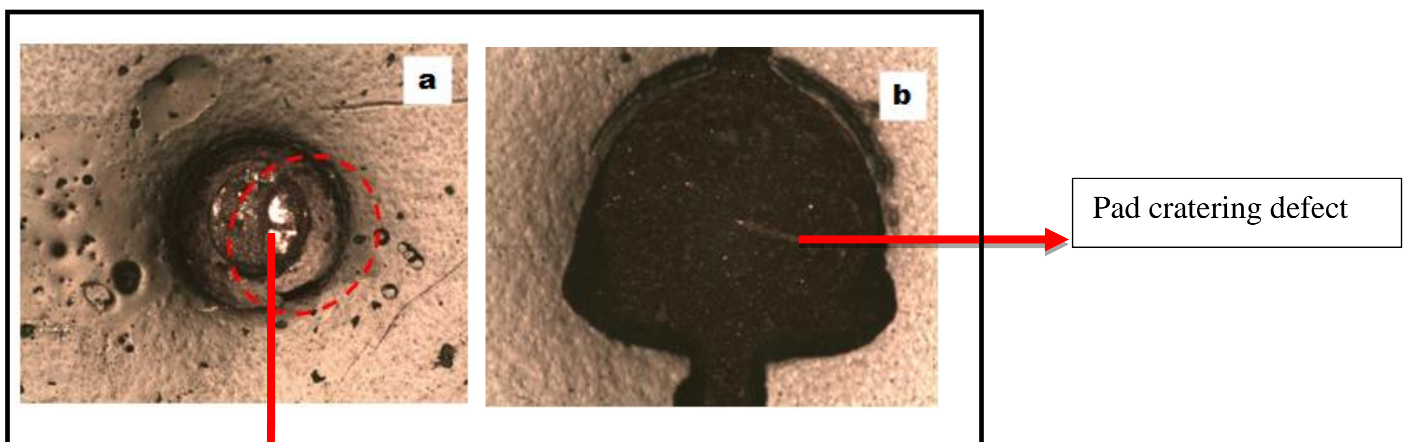

Figure 34 - a) L23+Sn99CN/High temperature profile - Dual Failure Mode b) L27+SAC305/High temperature profile - Pad Cratering Failure

The sheared pad surface of high temperature reflow profile sample is analyzed in the optical microscope. Looking into the surface, we can say that the failure mode is dual failure (30% to 70% IMC). The three types of failure modes were discussed earlier in the experimental approach chapter 2. From this we can say that there is an improvement in the failure mode with the high temperature reflow process.

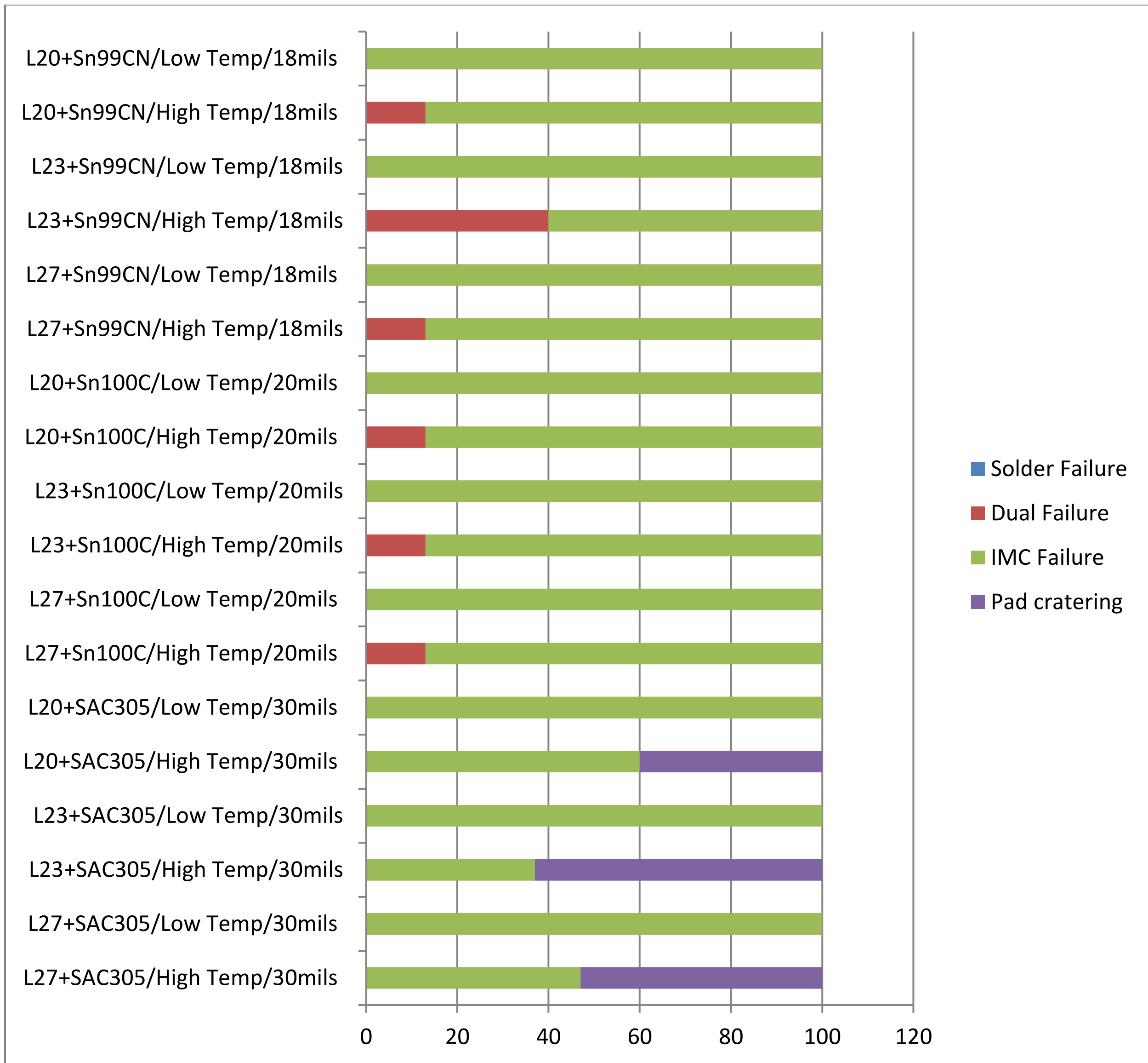

Figure 35 - Failure modes after reflow

The IMC growth evaluation along the solder substrate interface was also carried out on some set of cross-sectioned samples which are displayed in the Table 17 below. IMC growth thickness was using the ImageJ software.

In the after reflow condition, the IMC growth of the high temperature reflow process tends to be higher than the low temperature reflow process which is because the high temperature reflow

profile has higher zone temperatures than the low temperature reflow profile. As discussed earlier, the IMC grows faster in the higher temperature process than with the lower temperate process. Whereas in the aged condition, the IMC growth tends to be higher for the low temperature reflow process than for the high temperature reflow process which may be because of the homologous temperature. As the aging temperature of 125°C is relatively close to the melting temperature of SnBi paste 138°C, it has a significant impact on the IMC growth thickness.

	As-soldered Condition		Aged Condition	
	Low Temp Process (µm)	High Temp Process(µm)	Low Temp Process(µm)	High Temp Process(µm)
L20+SAC305	0.76	1.40	2.34	2.09
L23+Sn100C	0.79	1.60	2.01	1.83
L27+Sn99CN	0.78	1.50	3.26	1.85

Table 17- IMC growth comparison between as-soldered condition and aged condition

4.0 Chapter 4 - Conclusion

From the ball shear test, the high temperature reflow profile process resulted in a greater strength than low temperature reflow profile process. With the low temperature reflow process, the peak temperature (177ºC) is insufficient to melting and dissolve the lead free ball. The solder ball alloys used in the study have a melting point range from 215ºC to 227ºC. Incomplete mixing creates a high concentration of Bi precipitates in the high stress region of the shear test resulting in weak solder joint. Whereas with the high temperature reflow profile process, (peak reflow temperature 217ºC), the lead-free balls are able to more completely melt and coalesce with the SnBi paste (excluding Sn100C).

From the cross sectional analysis, for the low temperature reflow profile process there is no proper dissolution between the paste and ball, whereas with the high temperature reflow profile process, the paste and the ball are completely dissolved. The reason for this is the higher peak temperature in the high temperature reflow process. With L23 + Sn100C process, there is partial dissolution between the paste and the ball as the pasty range of L23 is very high and the Ag content in the ball tend to affect the dissolution.

From this study, a consistent improvement in high temperature assembly process is observed with the SAC305 solder paste. In addition, the results show a tighter distribution of the data for this alloy. Although an improvement in the Sn99CN and Sn100C was observed, its standard deviation of the results indicates a non-repeatable result and overlap in strength between the two processes.

Micro-alloying improvements in strength for the Sn99CN and Sn100C alloys seems to be limited. Addition of Cu and Ni in the L27 solder paste does not appear to have a comparable increase in strength as compared to SAC305. In fact, L23 (addition of 1wt%Ag) appears to provide the highest strength for the Sn99CN and Sn100C alloys in the high temperature process prior to and following aging.

From SEM/EDS analysis, for the low temperature process, high concentration of bismuth was found on the sheared surface. In the low temperature profile, the bismuth does not dissolve and the crack propagates through the weaker Bi grain boundaries and hence most of the defects are brittle IMC defects. Whereas for the high temperature reflow profile process the sheared surface has high concentration of tin, copper with very few percent of bismuth precipitates. Therefore, with the high temperature process the bismuth is able to dissolve well into the tin and give better strength.

The IMC growth thickness in the as-soldered condition is high for high temperature process than the low temperature process whereas in the aged condition the IMC growth is high for the low temperature process. This is because the aging temperature is relatively close to melting temperature of the SnBi paste. Therefore, the homologous temperature has an impact on the IMC growth thickness during aging condition.

Overall, from this investigation, some of the reasons for considering high temperature reflow profile process are improved shear strength, improved failure mode, slow IMC growth and less sensitivity to alloy variation. Thus, with the high temperature reflow process for the mixed solder alloy combinations, we can reduce the assembly processing temperature by which warpage can be reduced which improves yield, and we can improve the economic and environmental factors related to electronics assembly process.

Thus, this paper describes that by generating a robust high temperature reflow assembly process for SnBi low temperature solder paste, the cost can be reduced, failure modes can be improved and the shear strength can be increased, which may improve product yield in production.

References

[1] "Understanding Lead-free Electronics Packaging, Material Selection, Process, Defects, Reliability and Implementation," Center for Electronics Manufacturing and Assembly, Rochester Institute of Technology,, 2005.

[2] J. S. Hwang, "A Strong Lead-free Candidate: the Sn/Ag/Cu/Bi System," *Surface Mount Technology,* August 2000.

[3] L. Kondrachova, S. Aravamudhan, R. Sidhu and D. Amir, "Fundamentals of the Non-Wet Open BGA Solder Joint Defect Formation," in *International Conference on Soldering and Reliability (ICSR)*, 2012.

[4] R. Aspandiar, K. Byrd, T. Kok Kwan, L. Campbell and S. Mokler, "Investigation of Low Temperature Solders to Reduce Reflow Temperature, Improve SMT Yields and Realize Energy Savings," in *IPC APEX EXPO*, 2015.

[5] A. E. Schwaneke, W. L. Falke and V. R. Miller, "Surface Tension and Density of Liquid Tin-Lead Solder Alloys," *Journal of Chemical and Engineering Data,* vol. 23, no. 4, pp. 298-302, 1978.

[6] Z. Mei, J. W. Morris, M. C. Shine and T. E. Summers, "Effects of cooling rate on mechanical properties of near-eutectic tin-lead solder joints," *Journal of Electronic Materials,* vol. 20, no. 10, pp. 599-608, 1991.

[7] H. K. Charles and G. V. Clatterbaugh, "Solder Joint Reliability — Design Implications From Finite Element Modeling and Experimental Testing," *Journal of Electronic Packaging,* vol. 112, no. 2, pp. 135-146, June 01, 1990.

[8] M. Abtew and G. Selvaduray, "Lead-free solders in microelectronics," *Material Science Engineering,* vol. 27, pp. 95-141, 2000.

[9] *European Parliament Proposal for a Directive of the European Parliament and of the Council on Waste*

Electrical and Electronic Equipment and on the restriction of the use of certain hazardous substances in electrical and electronic equipment COM, (2000) .

[10] "Lead-free solder final report, NCMS Report 0401RE96," National Center for Manufacturing Sciences, Michigan, 1997.

[11] M. R. Harrison and J. H. Vincent, "IDEALS: Improved design life and environmentally aware manufacturing of electronics assemblies by lead-free soldering," in *12th Microelectronics and Packaging Conference, IMAPS, pp. 98–104*, Europe, Cambridge, 1999.

[12] "JEIDA - Report on research and development on lead-free soldering," Japan Electronic Industry Development Association, Tokyo , 2000.

[13] S. K. Kang, W. K. Choi, M. J. Yim and D. Y. Shih, "Studies of the mechanical and electrical properties of lead-free solder joints," *Journal of Electronic Materials,* vol. 31, pp. 1292- 1303, 2002.

[14] F. Zhu, Z. Wang, R. Guan and H. Zhang, "Mechanical Properties of a Lead-Free Solder Alloys," in *International Conference on Asian Green Electronics, IEEE*, 2005.

[15] J. Bath, C. Handweker and E. Bradley, "Reasearch update: Lead-free solder alternatives," *Circuits Assembly,* pp. 31-40, 2000.

[16] M. O. Alam, Y. C. Chan and K. C. Hung, "Interfacial reaction of Pb-Sn solder and Sn-Ag solder with electroless Ni deposit during reflow," *Journal of Electronic Materials,* vol. 31, no. 10, pp. 1117- 1121, 2002.

[17] K. Banerji and R. F. Darveaux, "Effect of aging on the strength and ductility of controlled collapse solder joints," in *Microstructures and Mechanical Properties of Aging Materials conference*, 1993, pp. 431–442.

[18] D. Suh, D. W. Kim, P. Liu, H. Kim, J. A. Weninger, C. M. Kumar, A. Prasad, B. W. Grimsley and H. B. Tejada, "Effects of Ag content on fracture resistance of Sn-Ag-Cu lead-free solders under high strain rate conditions," *Materials Science and Engineering:A,* Vols. 460-461, pp. 595-603, July 2007.

[19] R. S. Pandher, B. G. Lewis, R. Vangav and B. Singh, "Drop Shock Reliability of Lead-Free Alloys - Effect of Micro-Additives," in *Proceedings 57th Electronic Components and Packaging Technology (ECTC)*, Reno, May 29-June 1, 2007..

[20] G. Henshall, R. Healy and R. S. Pandher, "iNEMI Pb-free Alloy Alternatives Project Report: State of the Industry," in *SMTAI*, 2008.

[21] N. S. Liu and K. Lin, "Evolution of interfacial morphology of Sn-8.5Zn-0.5Ag-0.1Al-xGa/Cu system during isothermal aging," *Journal of Alloys and Compounds,* vol. 456, pp. 466-473., 2008.

[22] J. Liang, N. Dariavach, D. Shangguan, E. Subir, Y. C. Lee and C. P. Wong, "Metallurgy, processing and reliability of lead-free solder joint interconnections in micro electronic materials, Physics, mechanics, design and reliability packaging," Springer, 2007.

[23] D. Suraski and K. Seelig, "The Current Status of Lead-Free Solder Alloys," *IEEE transactions on Electronics Packaging Manufacturing,* vol. 24, no. 4, October 2001.

[24] K. Suganuma, K. Niihara, T. Shoutoku and Y. Nak, "Wetting and interface microstructure between Sn-Zn binary alloys and Cu," *Journal of Materials Research,* vol. 13, pp. 2859- 2865, 1998.

[25] D. Q. Yu, H. P. Xie and L. Wang, "Investigation of interfacial microstructure and wetting property of newly developed Sn-Zn-Cu solders with Cu substrate," *Journal of Alloys and Compounds,* vol. 385, pp. 119-125, 2004.

[26] H. Wang, F. Wang, F. Gao, X. Ma and Y. Qian, "Reactive wetting of Sn0.7Cu-xZn lead-free solders on Cu

substrate," *Journal of Alloys and Compounds,* vol. 433, pp. 302-305, 2006.

[27] B. Sandy, E. Briggs and R. Lasky, "smtnet," Indium Corporation, may 2011. [Online]. Available: https://www.smtnet.com/library/files/upload/advantages_of_bismuth_based_alloys_for_low_temp_soldering.pdf.

[28] J.-W. Yoon, C.-B. Lee and S.-B. Jung, "Interfacial Reactions Between Sn-58mass%Bi Eutectic Solder and (Cu,Electroless Ni-P) Substrate," *Materials Transactions,* vol. 43, no. 8, pp. 1821-1826, 2002.

[29] Y. Zheng, C. Hillman and P. McCluskey, "Intermetallic Growth on PWBs Soldered with Sn 3.8Ag0.7Cu," in *Proceedings of ECTC*, San Diego, 2002.

[30] M. Sampathkumar, S. Rajesnayagham, P. S. Manian and P. J. Anson(P.E), "Investigation of the Performance of SAC and SAC-Bi Lead-Free Solder Alloys with OSP and Immersion Silver PCB Finishes," *SMTA Intenational,* 2005.

[31] S. Ngoh, W. Zhou, H. L. Pang and X. Shi, "Growth of Intermetallic Compounds during Isothermal Annealing of a Sn-Ag-Cu Lead-free Solder," *Soldering & Surface Mount Technology,* 2004.

[32] J. M. Juarez, M. Robinson, J. Heebink, P. Snugovsky, E. Kosiba, J. Kennedy, Z. Bagheri, S. Suthakaran and M. Romansky, "Reliability Screening of Lower Melting Point Pb-Free Alloys Containing Bi," in *IPC APEX*, 2013.

[33] N. Vijayaragavan, F. P. Carson and A. Mistry, "Package-on-Package Warpage–Impact of Surface Mount Yields and Board Reliability," in *ECTC*, 2008.

[34] P. Garrou, "Warpage in Microelectronic Packaging: a closer look," *Chip Scale Review,* pp. 5, Volume 18, No 4, , July 2014.

[35] H. Ma, J. C. Suhling, Y. Zhang, P. Lall and M. J. Bozack, "The Influence of Elevated Temperature Aging on

Reliability of Lead-free Solder Joints," *Electronic Components and Technology Conference,* 2007.

[36] R. Pandher and R. Healey, "Reliability of Pb-Free Solder Alloys in Demanding BGA and CSP Applications," in *Electronic Components and Technology Conference*, 2008.

[37] M. Mccormack, H. Chen, G. Kammlott and S. Jin, "Significantly Improved Mechanical Properties of Bi-Sn Solder Alloys by Ag-Doping," *Journal of Electronic Materials,* vol. 26, no. 8, pp. 954 - 958, August 1997.

[38] V. Schroeder, F. Hua and J. Gleason, "STRENGTH AND FATIGUE BEHAVIOR OF JOINTS MADE WITH Bi-42Sn-1Ag SOLDER PASTE: AN ALTERNATIVE TO Sn-3.5Ag-0.7Cu FOR LOW COST CONSUMER PRODUCTS," in *SMTA International*, 2001.

[39] V. Liu, J. Keck, E. Page and N.-C. Lee, "Voiding and Reliability of BGA Assemblies with SAC and 57Bi42Sn1Ag Alloys," in *SMTA*, China East - NEPCON Shanghai, 2014.

[40] J.-W. Yoon, S.-W. Kim and S.-B. Jung, "IMC Growth and Shear Strength of Sn-Ag-Bi-In/Au/Ni/Cu BGA Joints During Aging," *Materials Transactions,The Japan Institute of Metals and Materials,* vol. 45, no. 3, p. 727 to 733, 2004.

[41] E. Bradley, C. A. Handwerker, J. Bath, R. D. Parker and R. W. Gedney, Lead-Free Electronics: iNEMI Projects Lead to Successful Manufacturing, Wiley-IEEE Press, October 2007.

[42] M. Li, H. Xu, J. Kim and H. Kim, "Failure Modes of Lead-free Solder Bumps Formedby Induction Spontaneous Heating Reflow," *Journal of Materials Science and Technology,* vol. 23, no. 1, 2007.

[43] M. Li, K. Y. Lee, D. R. Olsen, W. T. Chen, B. T. Chong Tan and S. Mhaisalkar, "Microstructure, Joint Strength and Failure Mechanisms of SnPb and Pb-free Solders in BGA Packages," *IEEE Transactions on Electronics Packaging,* vol. 25, no. 3, 2002.

[44] A. F, S. H, S. D and C. P, "A Shear Strength Study on Lead-Free Solder Spheres for BGA Applications on Different Pad Finishes," in *Pan Pacific Microelectronics Symposium, SMTA, pp 11-28*, 2001.

[45] T. Siewert, J. Madeni and S. Liu, "Formation and Growth of Intermetallics at the Interface Between Lead-free Solders and Copper Substrates," in *APEX*, 1994.

[46] The Data Visualisation Catalogue http://www.datavizcatalogue.com/methods/box_plot.html

[47] T. Siewert, J. Madeni and S. Liu, "Formation and Growth of Intermetallics at the Interface Between Lead-free Solders and Copper Substrates" in APEX, 1994.

[48] Craig Freudenrich, “How Light Microscopes Work” in HowStuffworks http://science.howstuffworks.com/light-microscope1.htm

[49] Jonathan Atteberry, “The Key Components of a Scanning Electron Microscope” in HowStuffworks http://science.howstuffworks.com/scanning-electron-microscope2.htm